DESIGN AND SIMULATION OF ALL-CMOS TEMPERATURE-COMPENSATED g_m-C BANDPASS FILTERS AND SINUSOIDAL OSCILLATORS

A Thesis

Presented to

The Graduate Faculty of The University of Akron

In Partial Fulfillment

of the Requirements for the Degree

Master of Science

Purushottam Parajuli

August, 2011

DESIGN AND SIMULATION OF ALL-CMOS TEMPERATURE-COMPENSATED

g_m-C BANDPASS FILTERS AND SINUSOIDAL OSCILLATORS

Purushottam Parajuli

Thesis

Approved:

Co-Advisor
Dr. Joan E. Carletta

Co-Advisor
Dr. Robert J. Veillette

Committee Member
Dr. Kye-Shin Lee

Accepted:

Department Chair
Dr. Alex De Abreu-Garcia

Dean of the College
Dr. George K. Haritos

Dean of the Graduate School
Dr. George R. Newkome

Date

ABSTRACT

This thesis presents a design method for the temperature compensation of operational transconductance amplifiers (OTAs) using temperature-dependent voltage sources. The transconductance value of an OTA is compensated by making the tail current of the OTA increase with temperature in such a way as to compensate the decrease in carrier mobility in the input transistors. The temperature-compensated OTAs are used to design tuned pairs of bandpass filters and sinusoidal oscillators using the standard g_m-C technique. The transistor-level circuits of tuned pairs of bandpass filters and sinusoidal oscillators are designed and simulated. The variations in the frequency characteristics of the pairs are less than 6% over the temperature range from 25°C to 125°C. The frequency characteristics are sensitive to process variations; however, the center frequency of the bandpass filter and the frequency of oscillation of the sinusoidal oscillator change in same direction and the pairs remain tuned within 6% at all process corners.

ACKNOWLEDGEMENTS

First of all, I would like to thank my advisors Dr. Joan Carletta and Dr. Robert Veillette, for their guidance, encouragement and support throughout my graduate studies and my research work. Their insight into the circuit design and their energy and focus has inspired me a lot. I feel extremely privileged to be associated with them and shall always be grateful to them.

I would also like to thank my committee members, Dr. Firas Hasan and Dr. Kye-Shin Lee, for their time and valuable comments on my research.

I take this opportunity to thank my wife Lalita for her support, help and encouragement at every hurdle. Finally, I would like to thank my parents for their constant love and encouragement throughout my life.

TABLE OF CONTENTS

LIST OF TABLES

LIST OF FIGURES

CHAPTER I

INTRODUCTION

1.1 Motivation

Bandpass filters and sinusoidal oscillators are two important components of mixed-signal circuits. Bandpass filters may be used in signal modulation and demodulation in applications that use Frequency-Division Multiple Access (FDMA) communication. Sinusoidal oscillators may be used in a variety of electronic applications such as radio transmitters and receivers.

Bandpass filters and sinusoidal oscillators may be used as tuned pairs in frequency multiplexing signals from several sensors. An example of such an application is shown in Figure 1.1. The system consists of n sensors whose outputs are amplitude-modulated at different frequencies using n separate oscillators. The modulated outputs are frequency-division multiplexed and transmitted through a single analog communication channel. At the receiving end, the transmitted signal is applied to n separate bandpass filters, each of which is tuned to the frequency of one of the oscillators. The outputs of the individual sensors can be recovered at the receiving end using envelope detection of the outputs from the individual bandpass filters.

For applications such as these, the center frequency of the bandpass filter and the frequency of oscillation of the sinusoidal oscillator are required to be tuned to the same

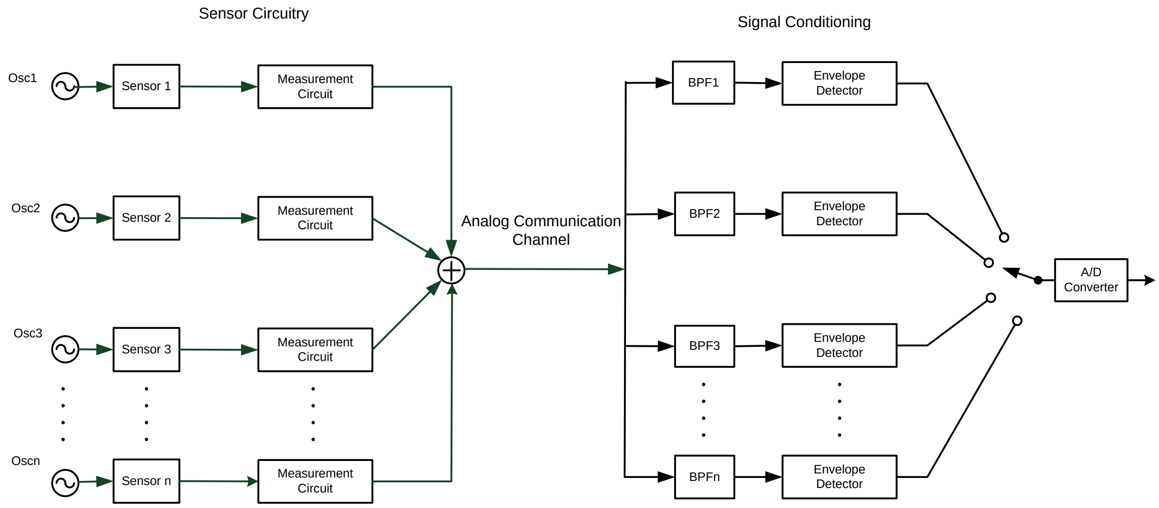

Figure 1.1 Application for tuned bandpass filters and sinusoidal oscillators.

frequency. For high-temperature applications, such as sensors in an industrial process, the bandpass filters and sinusoidal oscillators may be required to remain tuned over a range of temperatures. They should also be well tuned despite process variations in the fabrication of the integrated circuits.

1.2 Goal of the thesis

The primary goal of the current thesis work is to design tuned pairs of bandpass filters and sinusoidal oscillators which can be implemented in a high-temperature multi-channel sensor interface integrated circuit. The bandpass filters and sinusoidal oscillators must remain tuned at their respective frequencies over a temperature range of 25°C to 125°C. The design also must work despite process variations, in the sense that the frequency characteristics of the bandpass filters and sinusoidal oscillators must change in the same way with the process variations. If so, a filter and an oscillator fabricated together on one chip may be separated and used in different environmental conditions and still operate as a tuned pair.

Conventional filter and oscillator designs use active components such as operational amplifiers [1, 2]. In these designs, the maximum frequency of operation is limited to the gain-bandwidth product of the operational amplifier, which is typically no more than a few megahertz. In addition, they may require resistive, capacitive, or inductive components that must be implemented off chip.

In this thesis, we design frequency-tuned second-order bandpass filters and second-order sinusoidal oscillators using the standard g_m-C technique [3]. The g_m-C circuit designs use high-output-resistance operational transconductance amplifiers (OTAs) and capacitive elements connected as their loads. The advantage of the g_m-C technique is that the bandpass filters and oscillators can be built on a single chip and they can operate over a wide range of frequencies, from a few hertz to a few gigahertz. The frequency characteristics of the circuits are determined by the magnitudes of the OTA transconductances and of the capacitive loads. The frequency tuning of bandpass filters and sinusoidal oscillators can be achieved by using the same pairs of OTAs in determining the frequencies of both.

In this thesis, the g_m-C technique is extended to make the bandpass filters and sinusoidal oscillators insensitive to temperature. The transconductance of an OTA decreases with temperature because of reduced carrier mobility. The temperature compensation of an OTA is achieved by making the bias currents of the amplifying devices increase with temperature in such a way as to compensate the decrease in carrier mobility and maintain a constant transconductance. The increase in bias current with temperature is achieved using a temperature-dependent voltage source.

1.3 Summary of contribution

A design method for the temperature compensation of an OTA using an all-CMOS temperature-dependent voltage source is introduced. The transistor-level circuits of temperature-compensated tuned pairs of bandpass filters and sinusoidal oscillators are designed using the proposed method. The bandpass filter center frequencies and the oscillator frequencies are both shown in simulation to vary less than 6% over the temperature range from 25°C to 125°C. Thus, ignoring any effect of process variations, the bandpass filter and the sinusoidal oscillator of a tuned pair would have a frequency mismatch of no more than 6% even if the two were operated in different temperature environments.

The frequency characteristics of the designed OTAs are affected by process variations; however, because the bandpass filters and the sinusoidal oscillators are built from matched OTA designs, the process variations effects on both are similar and the pairs tend to remain tuned. The mismatch between the bandpass filters and the sinusoidal oscillators is less than 6% at all process corners. Therefore, assuming there is no process variation across the wafer, if the tuned pairs of bandpass filters and sinusoidal oscillators are fabricated on one wafer and then separated to work in different temperature environments, the total mismatch in their frequency characteristics will be no more than 12%.

A low-frequency bandpass filter requires either a low transconductance value or a high capacitance value. In this thesis, a capacitor-multiplier circuit is designed which is used to multiply a 1-pF capacitor by a factor of 10 to obtain a 10-pF equivalent capacitance. A 40-kHz bandpass filter is first designed and simulated using an ideal capacitor. Then, it is simulated using the capacitance obtained from the capacitor-multiplier circuit. The center frequency of the filter is shown in simulation to vary 0.6 kHz, or 1.5%, from the center frequency of the filter using an ideal capacitor. The center frequency of the filter is shown to vary less than 6% over the temperature range from 25°C to 125°C.

The OTA circuits are known generally to be sensitive to temperature, and they have been restricted to use in an environmentally controlled condition [4]. Temperature compensation of OTAs is known to be achieved by using external components [4, 5] or by using multiple OTAs with external components [6]. In this thesis, temperature compensation of OTAs is achieved without using any external components. The proposed method uses all-CMOS temperature-dependent voltage sources to temperature-compensate the OTAs. The temperature-compensated OTAs are then used to design bandpass filters and sinusoidal oscillator to form tuned pairs.

1.4 Organization of the thesis

The rest of this thesis is divided into four chapters. In Chapter II, various architectures of bandpass filter and oscillator designs are presented along with their advantages and disadvantages. Previous work on achieving constant transconductance circuits is discussed. A capacitor-multiplier circuit [7] used to multiply a capacitor is introduced and designed. In Chapter III, the design method for the proposed tuned bandpass filters and sinusoidal oscillators is introduced along with the design of an all-CMOS temperature-dependent voltage source. In Chapter IV, the simulation results of the circuits designed by the proposed method are shown. In Chapter V, the results are summarized and possible future work is discussed.

CHAPTER II

BANDPASS FILTER AND SINUSOIDAL OSCILLATOR DESIGN BACKGROUND

Bandpass filters and sinusoidal oscillators can be implemented using different architectures. In this chapter, several different bandpass filter and sinusoidal oscillator architectures are presented. Special emphasis is given to the g_m-C circuits, which can operate over a wide range of frequencies and can be fabricated on an integrated circuit. The design and operation of different transconductors that may be used in g_m-C circuits are presented and explained. A discussion of temperature-insensitive and temperature-compensated transconductor circuits is also given. Finally, a capacitor-multiplier circuit [7] that is useful in reducing the layout area of a g_m-C circuit is analyzed.

2.1 Bandpass filter architectures

Bandpass filters allow signals in a certain frequency range to pass while rejecting signals outside this range. The transfer function of a standard second-order bandpass filter is given by

$$H(s) = \frac{G\frac{\omega_0}{Q}s}{s^2 + \frac{\omega_0}{Q}s + {\omega_0}^2}$$

where ω_0 is the center frequency, G is the gain at the center frequency and Q is the quality factor of the filter. The quality factor is given by

$$Q = \frac{\omega_0}{BW}$$

where BW is the bandwidth of the bandpass filter. Figure 2.1 shows the frequency response of a bandpass filter, showing ω_0, G and BW.

Bandpass filter architectures are classified on the basis of whether they are made from passive or active components. Passive bandpass filters are made using only resistors, inductors and capacitors, while active bandpass filters also include amplifying elements such as transistors in addition to passive components. The structure and operation of both passive and active bandpass filters are explained in the following subsections.

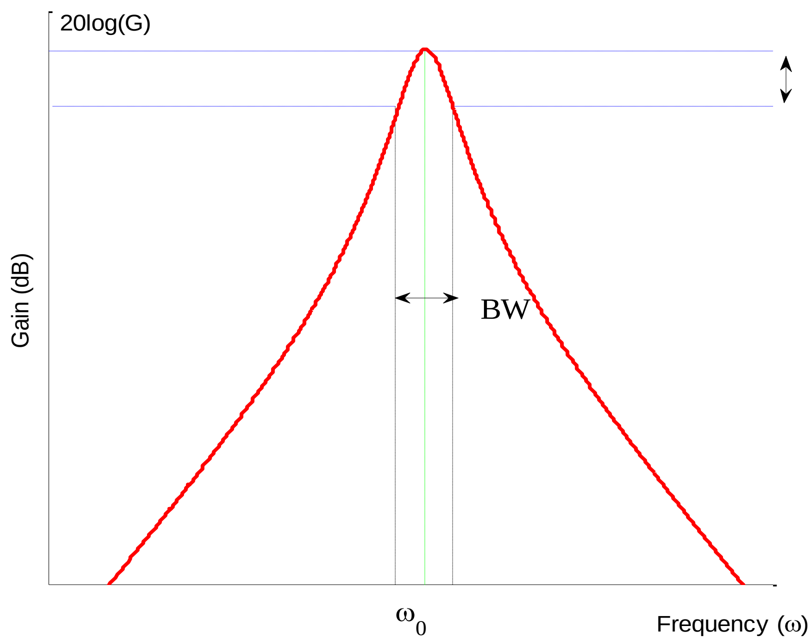

Figure 2.1 Frequency response of a second-order bandpass filter

2.1.1 Passive bandpass filters

Passive bandpass filters employ passive components to synthesize the filter structure [8]. Figure 2.2 shows a second-order RLC bandpass filter, which is one of the simplest and most common passive bandpass filter architectures. The transfer function of this circuit is given by

$$\frac{v_{out}(s)}{v_{in}(s)} = \frac{\frac{R}{L}s}{s^2 + \frac{R}{L}s + \frac{1}{LC}}.$$

For this bandpass filter, the center frequency is $\omega_0 = \sqrt{\frac{1}{LC}}$, the gain at the center frequency is $G = 1$, and the quality factor, which is the ratio of the center frequency to the bandwidth, is $Q = \sqrt{\frac{L}{R^2C}}$. The center frequency can be set by choice of the inductor and capacitor values. The quality factor can then be set by choice of the resistor value without affecting the value of the center frequency.

Passive bandpass filters require no power supplies and can work well at very high frequencies. They can also be used in applications involving larger current or voltage levels. However, they cannot provide power gain to the input signals, and therefore may need a separate gain stage for amplification. In addition to this, inductors are necessary for any high-quality-factor passive bandpass filters. Although it is possible to fabricate on-chip resistors and capacitors, techniques for fabricating precise on-chip inductors are still in early stages of development [9]. Therefore, passive bandpass filters

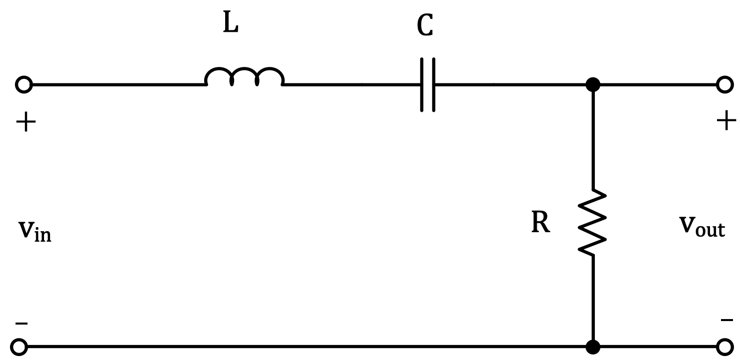

Figure 2.2 A passive bandpass filter

cannot easily be built entirely on chip, without external components. For this reason, we will not consider them further.

2.1.2 Active bandpass filters

Active bandpass filters utilize transistors, sometimes in the form of operational amplifiers or sometimes in the form of operational transconductance amplifiers, to synthesize the filter structure. Active bandpass filters require no inductors and are therefore more easily implementable in integrated circuits than passive bandpass filters. Active RC filters and g_m-C filters are two of the most common types of active bandpass filters. An active RC filter uses an operational amplifier with resistors and capacitors in its feedback network. A g_m-C filter uses only transconductors and capacitive elements connected as loads, and has the advantage that it requires no resistors. Active RC bandpass filters and g_m-C bandpass filters are discussed in the following subsections.

(A) Active RC bandpass filter

In an active RC bandpass filter, the desired frequency response is achieved by the use of an operational amplifier along with resistive and capacitive components. Figure 2.3 shows a second-order Sallen-Key bandpass filter structure, which is one of the most popular active RC bandpass filter architectures [1]. In this architecture, a non-inverting amplifier is used with feedback resistors and capacitors which cause the structure to operate as a bandpass filter. The transfer function of this bandpass filter can be found as

$$\frac{v_{out}(s)}{v_{in}(s)} = \frac{\left(1+\frac{R_b}{R_a}\right)\frac{s}{R_1C_1}}{s^2+\left(\frac{1}{R_1C_1}+\frac{1}{R_2C_1}+\frac{1}{R_2C_2}-\frac{R_b}{R_aR_fC_1}\right)s+\frac{R_1+R_f}{R_1R_2R_fC_1C_2}}\ .$$

The center frequency of this bandpass filter is $\omega_0 = \sqrt{\frac{R_f+R_1}{R_1R_2R_fC_1C_2}}$, the gain at the center frequency is $G = \frac{1+\frac{R_b}{R_a}}{1+\frac{R_1}{R_2}+\frac{R_1C_1}{R_2C_2}-\frac{R_bR_1}{R_aR_f}}$ and the quality factor is

$$Q = \frac{\sqrt{R_1R_2C_1C_2\left(1+\frac{R_1}{R_f}\right)}}{R_1C_1+R_1C_2+\left(1-\frac{R_bR_1}{R_aR_f}\right)R_2C_2}.$$

A Sallen-Key bandpass filter is easy to implement, and its center frequency, bandwidth and gain can be set by simply adjusting the values of the resistors and capacitors. However, its performance at higher frequencies is limited by the gain-bandwidth product of the operational amplifier, which is typically no more than a few megahertz. In addition, to eliminate off-chip components, the circuit requires the use of

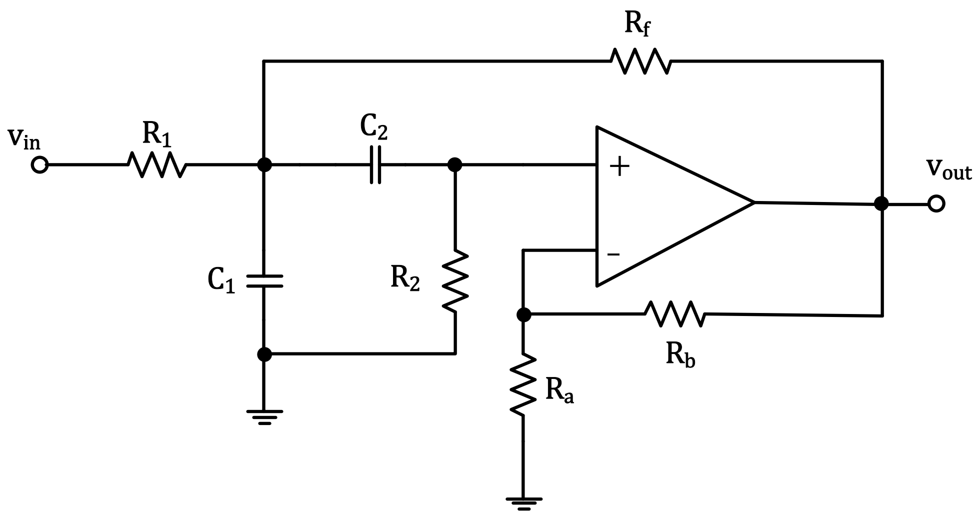

Figure 2.3 A Sallen-Key active RC bandpass filter

integrated-circuit resistors, which consume a large area. For these reasons, active-RC bandpass filters are not considered for the design.

(B) g_m-C bandpass filter

An alternative kind of active bandpass filter is based on operational transconductance amplifiers (OTAs) and capacitors [3, 10]. An OTA is a differential-input transconductor. Figure 2.4 shows the symbol of an OTA with inputs v_+ and v_-. The output current of this OTA is given by $i_{out} = g_m(v_+ - v_-)$, where g_m is the transconductance value of the OTA. An OTA is required to exhibit high input impedance and high output impedance. An OTA provides a constant output current for a given input voltage as long as the load connected to the output terminal has sufficiently low impedance compared to output impedance of the OTA.

An OTA can be used to form integrators and resistors, which may then be used in bandpass filter and oscillator architectures. Figure 2.5 shows an OTA with a capacitive load and one input connected to the ground, used to form an integrator. In this circuit, for a given input voltage v_{in}, the output voltage is $v_{out} = \frac{g_m}{C}\int v_{in}dt$. Figure 2.6 shows an OTA used to form a resistor. The circuit consists of voltages v_A and v_B applied to the two inputs and a direct feedback connection. The output current to the circuit is $i_{OUT} = g_m(v_B - v_A)$; thus, viewed from the v_A terminal, the circuit appears as a resistance of $R = \frac{1}{g_m}$ between v_A and v_B. The circuit can be modified by reversing the two inputs of the OTA to form a negative resistor, which may be used in the construction of a sinusoidal oscillator.

Figure 2.7 shows a second-order g_m-C bandpass filter, which is the most common type of g_m-C bandpass filter. In this architecture, four different OTAs with different transconductances form a closed-loop structure to synthesize the bandpass filter. The transfer function of this bandpass filter can be found as

$$\frac{v_{bp}(s)}{v_{in}(s)} = \frac{-sg_{m1}C_2}{s^2C_1C_2 + sC_2g_{m2} + g_{m3}g_{m4}}.$$

For this bandpass filter, the center frequency is $\omega_0 = \sqrt{\frac{g_{m3}g_{m4}}{C_1C_2}}$, the gain at the center frequency is $G = \frac{-g_{m1}}{g_{m2}}$ and the quality factor is $Q = \sqrt{\frac{C_1}{C_2}}\frac{\sqrt{g_{m3}g_{m4}}}{g_{m2}}$. For given values of C_1 and C_2, the center frequency can be set by the choice of g_{m3} and g_{m4}. The quality factor can then be set by choice of g_{m2}, without affecting the value of the center frequency. Finally, the gain of the filter can be set by choice of g_{m1}, without affecting the quality factor or the center frequency.

Unlike active RC filters, g_m-C filters can operate at high frequencies. The design of a g_m-C filter is also very flexible, because the transconductance values of the OTAs can be adjusted by simple changes to the OTA circuit designs [8].

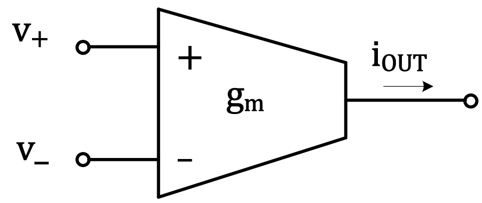

Figure 2.4 A simple OTA

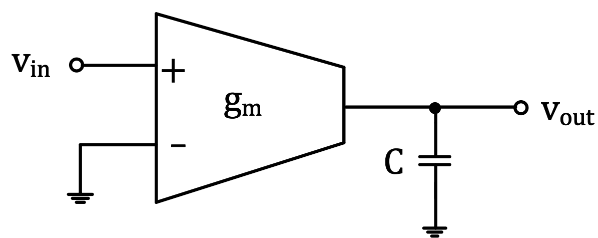

Figure 2.5 An OTA used to form an integrator

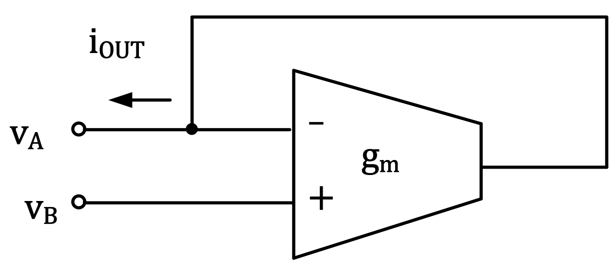

Figure 2.6 An OTA used to form a resistor

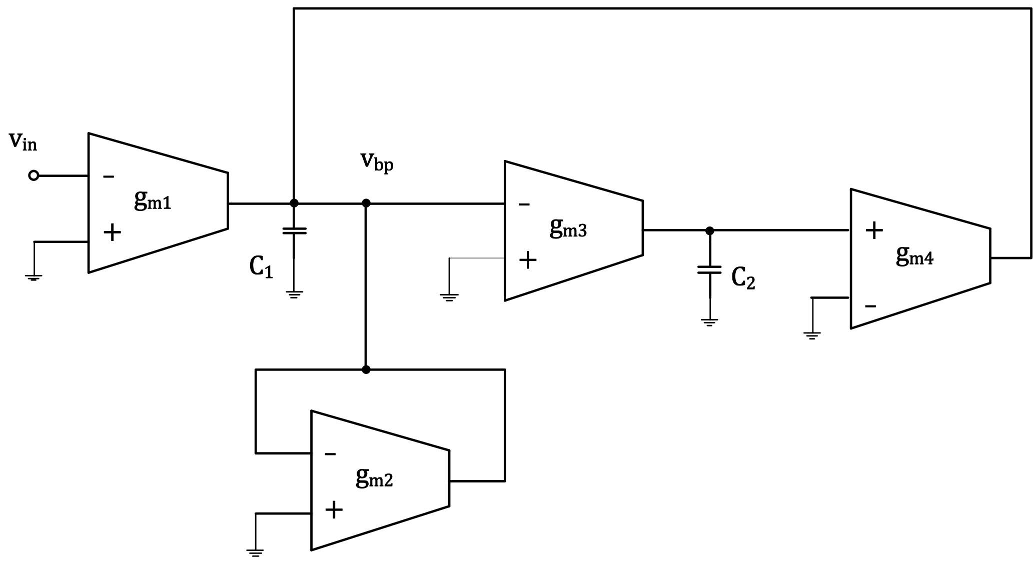

Figure 2.7 A second-order g_m-C bandpass filter

2.2 Sinusoidal oscillator architectures

Sinusoidal oscillators can be implemented using various techniques each having its own advantages and disadvantages. LC-tuned oscillators, RC oscillators and g_m-C quadrature oscillators are some of the most popular oscillators [2]. An LC-tuned oscillator consists of an active element and a combination of capacitors and inductors. An RC oscillator consists of an operational amplifier with a feedback network of resistors and capacitors ensuring the conditions for oscillation. A g_m-C quadrature oscillator utilizes OTAs and capacitive elements. The oscillator architectures are discussed in the following subsections.

2.2.1 LC-tuned oscillators

In LC-tuned oscillators, oscillation is achieved by a repeated conversion of electrostatic energy in capacitors to electromagnetic energy in inductors and vice versa [2]. Figure 2.8 shows a simplified schematic of a Hartley oscillator, which is the most common LC-tuned oscillator. The circuit consists of a feedback amplifier with a combination of a capacitor and two inductors. The resistor R is a model of losses in the inductors, the load resistance and the output resistance of the transistor. Assuming $\frac{1}{R} = 0$, the frequency of oscillation for this oscillator is given by $\omega_0 = \sqrt{\frac{1}{(L_1+L_2)C}}$.

A Hartley oscillator has a simple architecture, but the presence of two inductors makes it difficult to implement in an integrated circuit. Other LC tuned oscillator circuits include the Colpitts oscillator, the Armstrong oscillator and the Clapp oscillator [2], all of which have the same disadvantage. For this reason, LC-tuned oscillators are not considered further.

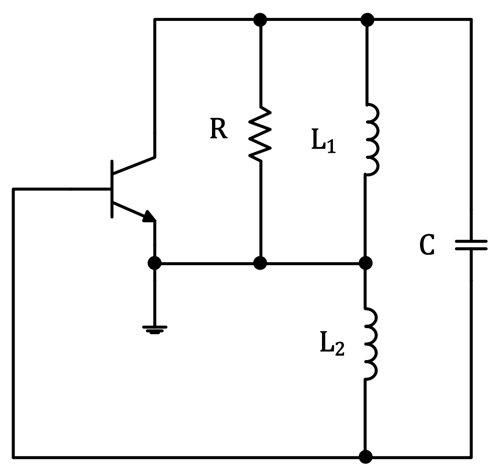

Figure 2.8 A Hartley LC-tuned oscillator

2.2.2 RC oscillators

In RC oscillators, the oscillation at a particular frequency is obtained by using operational amplifiers with RC networks. Figure 2.9 shows a schematic of a Wien bridge oscillator which is one of the simplest types of RC oscillator circuits. The circuit consists of an operational amplifier in a non-inverting configuration with an RC network for positive feedback. The resistor and capacitor values are chosen such that the feedback network transfer function has zero phase at the desired frequency of oscillation. The frequency of oscillation of this oscillator is given by $\omega_0 = \frac{1}{RC}$.

The Wien bridge oscillator is inexpensive and the frequency of oscillation can be selected by simply varying resistance values [2]. However, the frequency of oscillation is limited by the gain-bandwidth product of the amplifier. In addition to this, to eliminate off-chip components, the circuit requires the use of integrated-circuit resistors which occupy a large area. Other RC oscillators such as the phase-shift oscillator and the active-filter tuned oscillator [2] have similar disadvantages. For these reasons, the RC oscillators are not considered further.

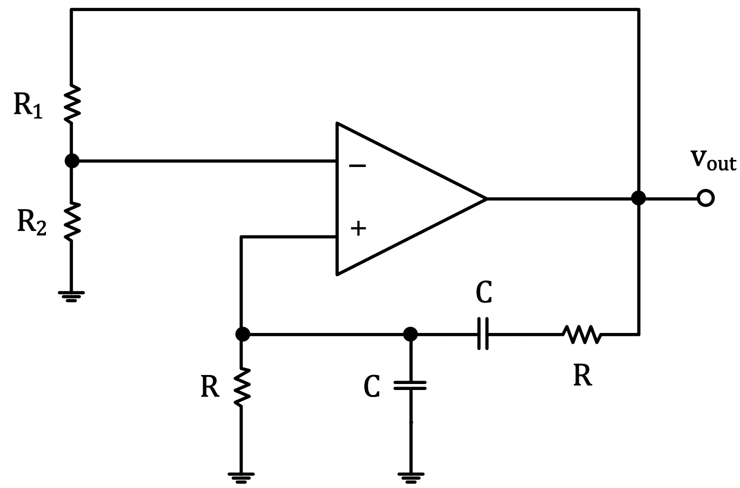

Figure 2.9 A Wien bridge RC oscillator

2.2.3 g_m-C quadrature oscillators

A g_m-C quadrature oscillator has an architecture similar to a g_m-C bandpass filter [11]. Figure 2.10 shows a simple g_m-C quadrature oscillator, which is one of the simplest g_m-C oscillators. The circuit produces two sinusoidal outputs v_{O1} and v_{O2} which are in quadrature (90 degrees out of phase), thus, getting its name "quadrature." The characteristic equation of the oscillator is given by

$$s^2 - \left(\frac{g_{mQ} - g_{m2}}{C_1}\right) s + \frac{g_{m3} g_{m4}}{C_1 C_2} = 0.$$

In this architecture, the transconductor g_{mQ} acts as a negative resistor. Its transconductance value is made slightly larger than g_{m2} to ensure oscillation. The frequency of oscillation is given by

$$\omega_0 = \sqrt{\frac{g_{m3} g_{m4}}{C_1 C_2}}.$$

In this architecture, the oscillation condition can be ensured by the choice of transconductors g_{mQ} and g_{m2} with minimal effect on the frequency of oscillation, which is determined by transconductors g_{m3} and g_{m4}.

The g_m-C sinusoidal oscillators have advantages and disadvantages similar to those of the g_m-C bandpass filters. Bandpass filters and sinusoidal oscillators designed using the g_m-C technique fit the best with the goal of the thesis in designing temperature-insensitive tuned bandpass filter and oscillator pairs that can operate over a wide range of frequencies and are easy to fabricate on an integrated circuit. Thus, this technique is used to design the bandpass filters and the sinusoidal oscillators in this thesis.

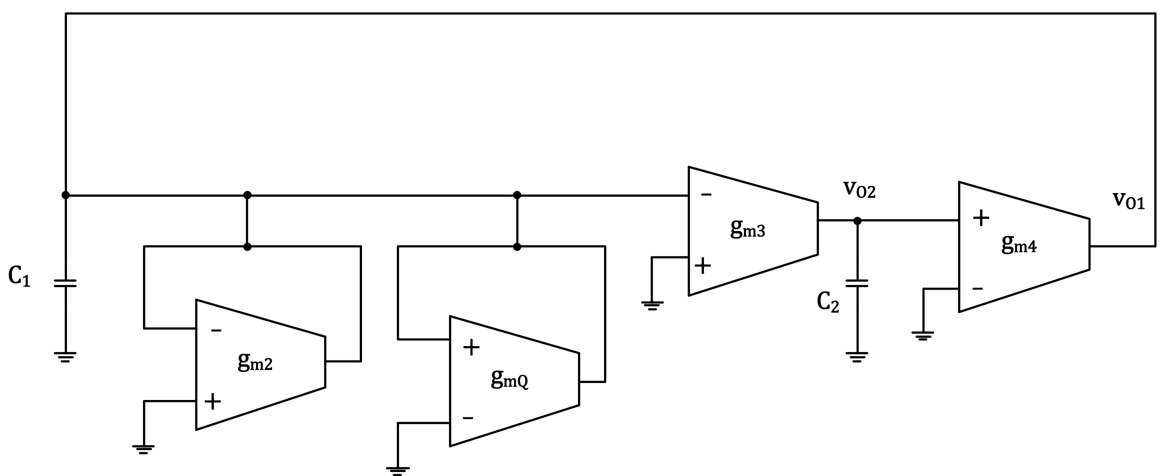

Figure 2.10 A g_m-C quadrature oscillator

2.3 Classification of transconductors

The main building block of g_m-C bandpass filters and sinusoidal oscillators is the transconductor. The architectures of transconductors are mainly classified based on the mode of input voltage. On this basis, transconductors can be classified as single-input or differential-input. The structure and operation of each of the two types are explained in the following subsections.

2.3.1 Single-input transconductors

In a single-input transconductor, the input voltage is applied to the gate of a single MOSFET and the output current is obtained through its drain terminal [3]. Figure 2.11 shows the schematic of a single-input negative transconductor which is one of the simplest types of single-input transconductor. It consists of a single MOSFET and a current source. The transconductance g_m of the MOSFET converts the change in the gate-to-source voltage (v_{in}) to a change in the current through the drain (i_d). The incremental output current i_{out} is negative of the incremental drain current i_d.

Single-input transconductors are easy to implement and require little chip area. However, they have a very low noise rejection [12]. They also have a small output current swing and limited output linearity [13]. The other single-input transconductors such as the cascode transconductor and the folded-cascode transconductor [14] have the same disadvantages. For these reasons, single-input transconductors are not considered further.

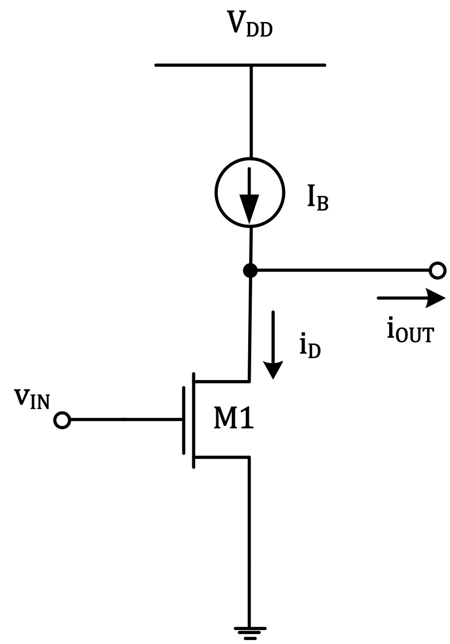

Figure 2.11 A single-input transconductor

2.3.2 Differential-input transconductors

Differential-input transconductors are popularly known as operational-transconductance-amplifiers (OTAs). Figure 2.12 shows the schematic of a balanced OTA [10], which is the most common type of OTA. The circuit consists of two input transistors M1 and M2, three current mirrors, M3-M4, M5-M6 and M7-M8, and a tail current source M9. The input voltage is applied between the gates of transistors M1 and M2. Through the three current mirrors, the drain currents of M1 and M2 are mirrored to transistors M8 and M4, respectively. The resulting output current i_{OUT} is the difference between the drain currents of the two input transistors. The transconductance value of the OTA is obtained as $g_m = \sqrt{\mu_n C_{ox} \frac{W}{L} I_{TAIL}}$, where W/L, C_{ox}, and μ_n are the channel aspect ratio, the gate oxide capacitance per unit area, and the charge-carrier mobility, respectively, of transistors M1 and M2. I_{TAIL} is the tail current through transistor M9.

OTAs have distinct advantages over single-input transconductors. Due to their differential input structure, they exhibit the property of common-mode noise rejection. OTAs also have larger output current swing and higher output linearity [13]. For these reasons, OTAs are considered for the further design.

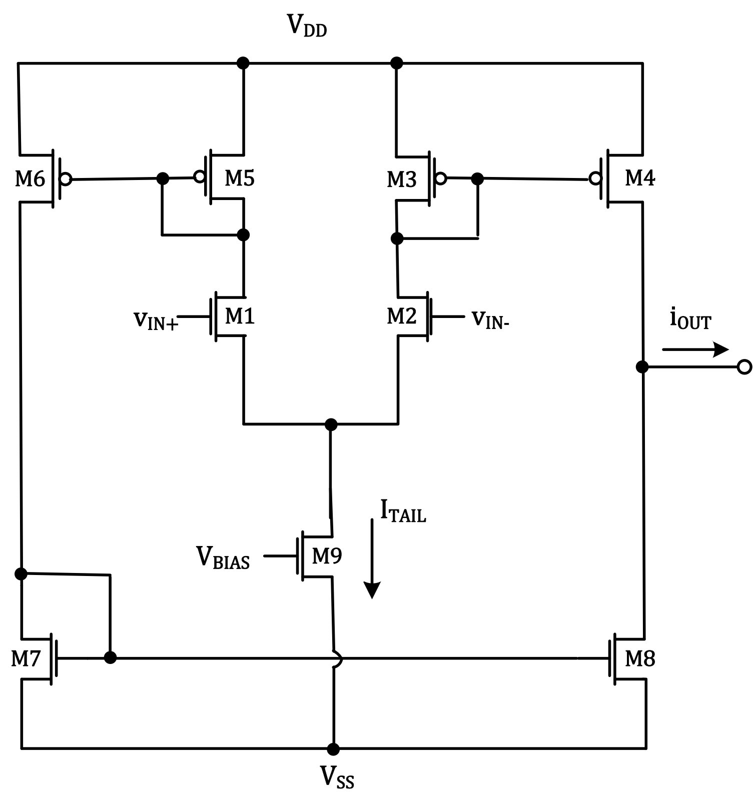

Figure 2.12 A balanced OTA, from [10]

2.4 Related work in temperature-insensitive g_m-C filter and oscillator design

Temperature-insensitive operation is one of the important design considerations in a g_m-C bandpass filter or oscillator design. Various techniques have been applied to ensure a better temperature performance of an OTA. A popular method for modifying an OTA to obtain a temperature-insensitive transconductance is shown in Figure 2.13 [6]. The circuit consists of two OTAs and a high-precision off-chip resistor. The OTA with transconductance value g_{m1} is designed as a resistor. The off-chip resistor is connected with this OTA to form a voltage divider. The voltage across the first OTA is applied as an input to the second OTA. It can be shown that the transconductance value of the equivalent temperature-compensated OTA is approximately $g_m = A_G \frac{1}{R}$, where the A_G is the ratio of transconductance values of the two OTAs. The resulting transconductance value is inversely proportional to the resistance value regardless of MOS process variations and power supply, voltage and temperature variations.

Talebbeydokhti [15] moved the off-chip resistor on chip to design a constant transconductance circuit; however, on-chip resistors typically have resistance values that are highly dependent on process variations and may occupy a large area. Gregoire and Un-Ku Moon [16] replaced the resistor by an on-chip switched capacitor network; however, this requires the use of a clock, and adds complexity and area to the design [17].

In this thesis, the transconductance of the OTA is compensated using a temperature-dependent voltage source. Figure 2.14 shows a BiCMOS temperature-dependent voltage source [12] which is a popular circuit to generate a temperature-dependent voltage that is proportional to absolute temperature (PTAT). The circuit consists of an $n:1$ MOS current mirror and two identical BJTs Q1 and Q2. It can be shown that the difference between the two base-emitter voltages, ΔV_{BE}, varies with temperature as $\Delta V_{BE} = \frac{kT}{q}\ln(n)$, where k is the Boltzmann constant, q is the charge of an electron and T is the absolute temperature. Thus, resulting ΔV_{BE} has PTAT voltage-temperature characteristics. However, the use of BJTs does not fit into the goal of this thesis; therefore, it is not considered for the design.

An all-CMOS temperature-dependent voltage source is used in [18]. The circuit uses transistors biased in weak inversion to obtain temperature-dependent voltage-temperature characteristics. This thesis uses a simpler circuit based on the one in [18] to design an all-CMOS temperature-dependent voltage source, which is then applied to the gate of the tail current source of the OTA. Thus, a temperature-insensitive OTA is achieved without external components. The design of a temperature-compensated bandpass filter and oscillator pair using a temperature-dependent voltage source to drive the tail currents is explained in detail in the following chapter.

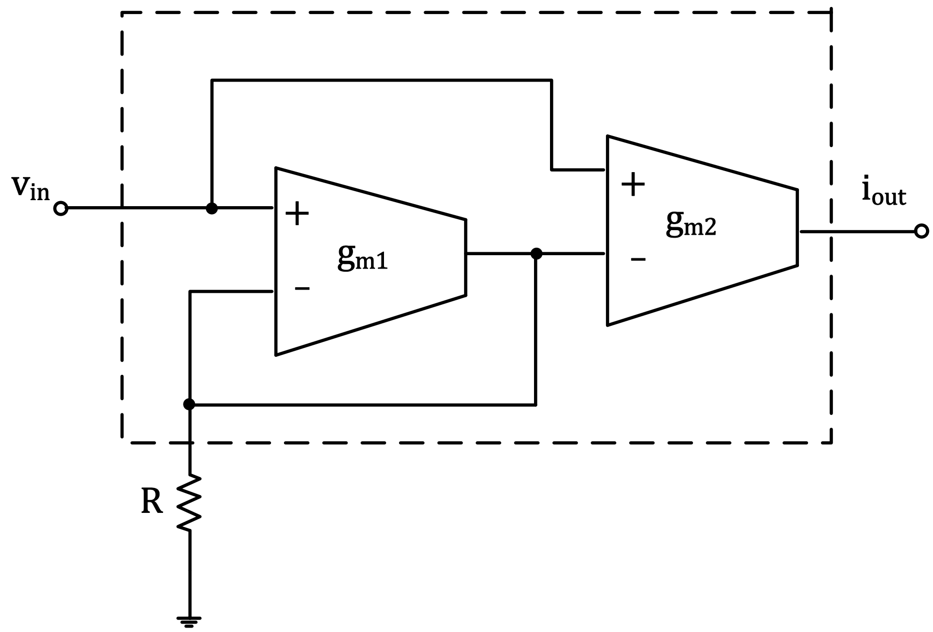

Figure 2.13 A temperature-compensated OTA using external resistor

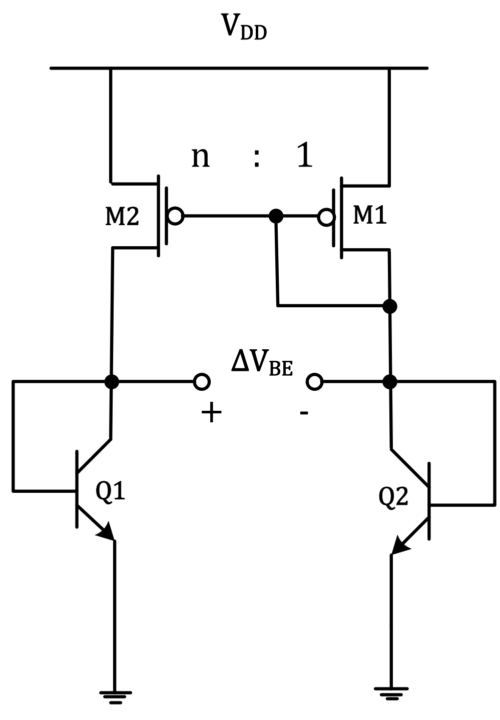

Figure 2.14 A BiCMOS PTAT voltage source

2.5 Capacitor-multiplier circuit

A capacitor-multiplier circuit plays an important role in integrated circuit design. The capacitors occupy a large chip area compared to transistors, and circuits requiring large capacitance values would require a large (and costly) IC chip. The design of a low-frequency filter or oscillator using the g_m-C technique would require either a low value of g_m [3] or a high value of capacitance. With a capacitor-multiplier circuit, low-frequency circuits can be designed using smaller values of capacitance.

Figure 2.15 shows a simple capacitor-multiplier circuit [7]. The circuit consists of a base capacitor C_i, whose capacitance is required to be multiplied, a bias current I_B which is generated by a diode-connected transistor MB, and two current mirrors M1-M2 and M3-M4. In addition to this, a cascode transistor MC is used in order to maintain a low noise level [7]. The circuit operates on the principle that if more current is produced by a given input voltage, the resultant circuit impedance is reduced. In the case of a capacitor, where the value of capacitance is inversely proportional to the impedance, the decrease in impedance would mean an effective increase in the capacitance value.

Figure 2.16 shows a small-signal equivalent of the circuit shown in Figure 2.15. It can be shown that, for $r_{o4} \gg \frac{1}{g_{mc}}$ and $r_{oc} \gg \frac{1}{g_{m1}}$, the small-signal impedance of the circuit is $z_{in}(s) = \frac{sC_i + g_{mc}}{\left[(N+1)C_i g_{mc} + \frac{1}{R}C_i\right]s + \frac{1}{R}g_{mc}}$, where R is the parallel equivalent resistance of r_{o2} and r_{o5} and N is the ratio of the W/L ratios of transistors M1 and M2. For $\frac{1}{NRC_i} \ll \omega \ll \frac{g_{mc}}{C_i}$, the circuit behaves approximately like a capacitor with capacitance of $(N+1)$ times the base capacitor C_i.

The capacitor-multiplier circuit is simulated using the design parameters shown in Table 2.1. In this design, a 1-pF capacitor is multiplied by a factor of 10 to obtain a 10-pF equivalent capacitance using the capacitor-multiplier circuit. With a sinusoidal input voltage of peak value 5 mV, the magnitude of the total current of the capacitor-multiplier circuit is measured over a frequency range of 1 kHz to 200 kHz. The phase is measured at a few points over the frequency range. Figure 2.17 and Figure 2.18 show these simulation results.

From Figure 2.17, it is observed that the capacitor-multiplier circuit behaves approximately as a 10-pF capacitor within the frequency range of 5 kHz to 100 kHz. The theoretical frequency range of capacitor-multiplier circuit operation is between $\omega \gg \frac{1}{NRC_i} = 4$ kHz and $\omega \ll \frac{g_{mc}}{C_i} = 2.5$ MHz.

It can be seen that, below 5 kHz, the admittance of the capacitor-multiplier circuit approaches a constant, implying the presence of a resistance in parallel with the equivalent capacitor. A model that is reasonably accurate for frequencies below 100 kHz can be constructed with a capacitor C and a parallel resistor R_P. Figure 2.19 shows this low-frequency circuit model of the capacitor-multiplier circuit. The value of the C is 10 pF and the parallel resistance R_P is approximately 8.7 MΩ. Figure 2.17 and Figure 2.18 show the magnitude and phase of the total current for both the simulated response and the low-frequency model. It is observed that the two magnitude plots overlap with one another and cannot be distinguished. A capacitor-multiplier circuit is used in this thesis to multiply a capacitor in a g_m-C bandpass filter.

Table 2.1 Design parameters for capacitor-multiplier circuit

g_{mc} (μA/V)	I_B (μA)	N	R (MΩ)	C_i (pF)	Measured capacitance (pF)	Theoretical capacitance (pF)
16	1	7	4.28	1.00	10.24	7.94

From the several different architectures presented in this chapter, the g_m-C technique is chosen for the design of bandpass filters and sinusoidal oscillators. The OTAs used in the design need to be temperature-compensated in order to have a temperature-insensitive operation of the g_m-C bandpass filters and sinusoidal oscillators. A design method to temperature-compensate an OTA is presented in Chapter III.

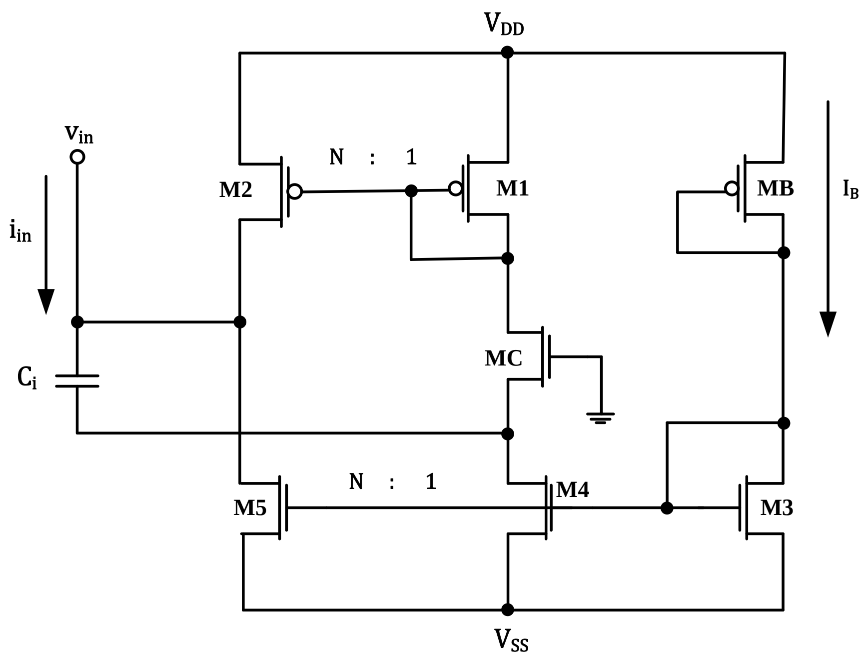

Figure 2.15 A capacitor-multiplier circuit

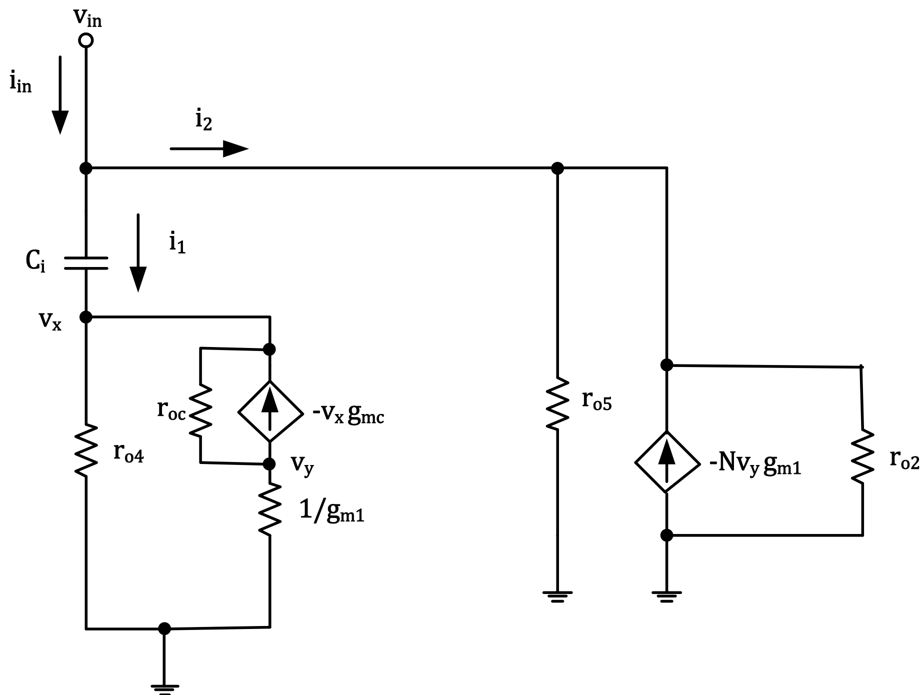

Figure 2.16 Small-signal model for the capacitor-multiplier circuit

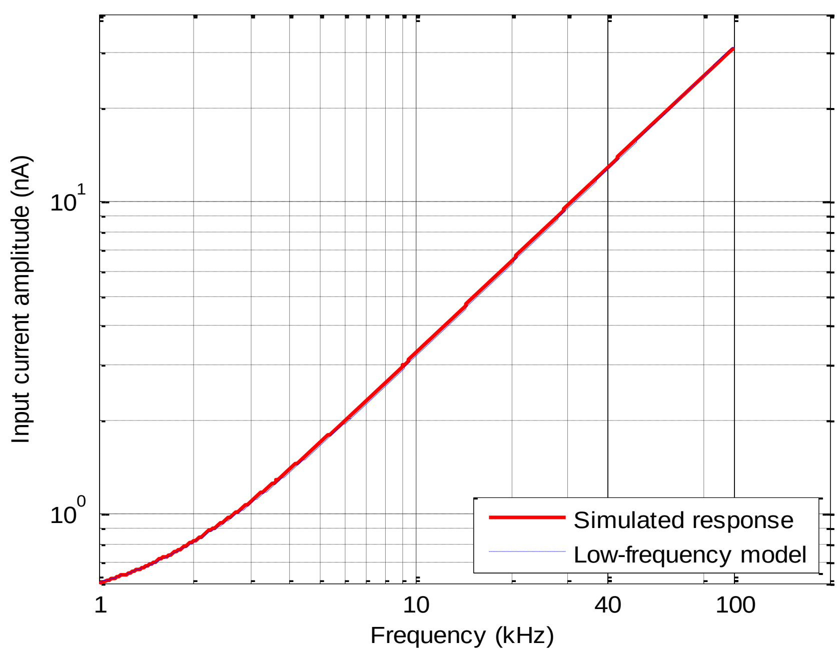

Figure 2.17 Magnitude response of capacitor-multiplier circuit

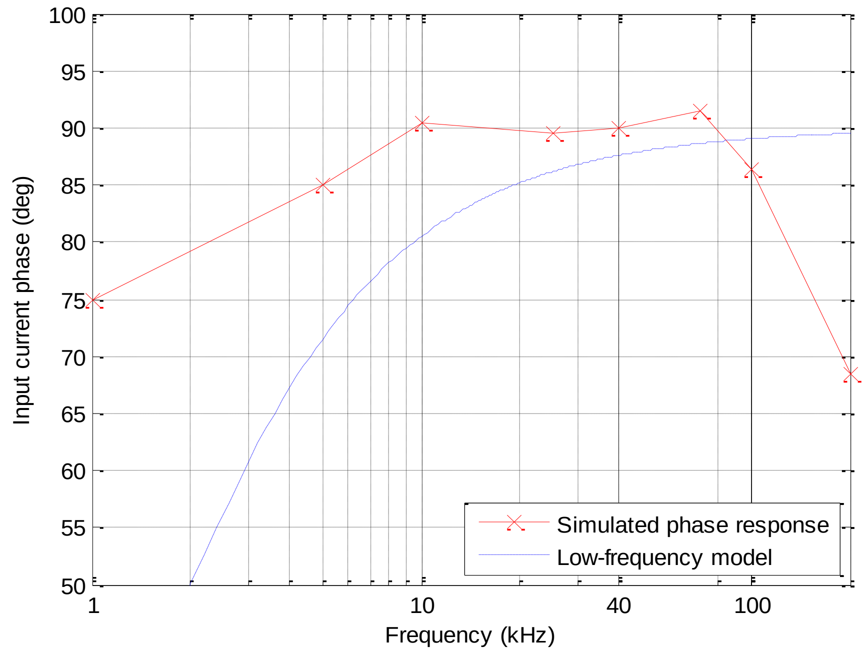

Figure 2.18 Phase response of capacitor-multiplier circuit

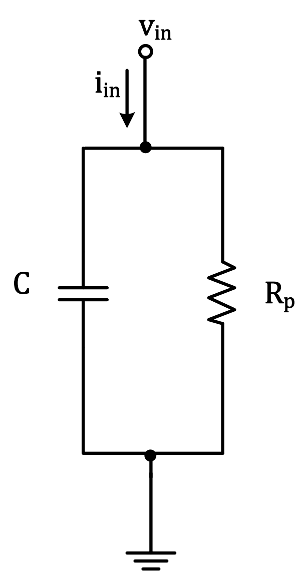

Figure 2.19 Low-frequency circuit model of capacitor-multiplier circuit

CHAPTER III

DESIGN OF TEMPERATURE-COMPENSATED OTA

In order to achieve temperature-insensitive operation of g_m-C bandpass filters and sinusoidal oscillators, the transconductances of the OTAs used in the design need to be temperature-insensitive. In this chapter, a design method is proposed for making the transconductance of an OTA temperature-insensitive by the use of an all-CMOS temperature-dependent voltage reference to modify the OTA tail current. Using the proposed design method, second-order bandpass filters and sinusoidal oscillators tuned in frequency are designed in a 0.5-μm silicon-on-insulator (SOI) process.

3.1 Temperature compensation for OTAs

The main component in both the bandpass filter and the oscillator, as well as in other g_m-C designs, is an OTA which is explained in Section 2.3.2, shown in Figure 2.12. The OTA produces an output current i_{OUT} proportional to the difference between the two input voltages v_{IN+} and v_{IN-} as

$$i_{OUT} = g_m(v_{IN+} - v_{IN-}). \qquad (3.1)$$

The transconductance g_m can be expressed as

$$g_m = \sqrt{\mu_n C_{ox} \left(\frac{W}{L}\right)_{1,2} I_{TAIL}}, \qquad (3.2)$$

where $\left(\frac{W}{L}\right)_{1,2}$, C_{ox}, and μ_n are the channel aspect ratio, the gate oxide capacitance per unit area and the charge-carrier mobility, respectively, of transistors M1 and M2. I_{TAIL} is the current through transistor M9. The tail current is given by

$$I_{TAIL} = \frac{1}{2}\mu_n C_{ox}\left(\frac{W}{L}\right)_9 (V_{GS} - V_T)^2, \tag{3.3}$$

where $\left(\frac{W}{L}\right)_9$, V_{GS} and V_T are the channel aspect ratio, the gate-to-source voltage and the threshold voltage, respectively, for the transistor M9.

The transconductance of the OTA and the tail current are a function of temperature T, because both the charge-carrier mobility and the threshold voltage may vary with temperature. Using subscript zeros to denote conditions at room temperature, the charge-carrier mobility μ_n depends on temperature as [19]

$$\mu_n(T) = \mu_{n0}\left(\frac{T}{T_0}\right)^{\alpha_\mu}, \tag{3.4}$$

where the exponent α_μ is negative and itself a function of temperature. For silicon, the empirical value of α_μ at room temperature is –1.5 to –2.1 [19]. The threshold voltage V_T depends on temperature as

$$V_T(T) = V_{T0} + \alpha_v(T - T_0), \tag{3.5}$$

where α_v is a negative constant with a typical value of -2.70 mV/°C. Thus, the tail current varies with temperature as

$$I_{TAIL}(T) = \frac{1}{2}\mu_{n0}\left(\frac{T}{T_0}\right)^{\alpha_\mu} C_{ox}\left(\frac{W}{L}\right)_9 [V_{GS} - V_{T0} - \alpha_v(T - T_0)]^2. \tag{3.6}$$

Considering the effects of temperature, the transconductance expression in (3.2) can be written as

$$g_m(T) = \sqrt{\mu_{n0}\left(\frac{T}{T_0}\right)^{\alpha_\mu} C_{ox}\left(\frac{W}{L}\right)_{1,2} I_{TAIL}(T)}, \tag{3.7}$$

where $I_{TAIL}(T)$is given by (3.6).

The decrease in charge-carrier mobility with temperature tends to decrease the transconductance of the OTA; this decrease in the transconductance with temperature can be compensated by making the tail current I_{TAIL} larger as temperature increases. In theory, the tail current that will exactly compensate for the decrease in charge-carrier mobility at temperature T is

$$\begin{aligned} I'_{TAIL} &= I_{TAIL0}\left(\frac{T}{T_0}\right)^{-\alpha_\mu} \\ &= \frac{1}{2}\mu_{n0}C_{ox}\left(\frac{W}{L}\right)_9 (V_{GS0} - V_{T0})^2\left(\frac{T}{T_0}\right)^{-\alpha_\mu}. \end{aligned} \tag{3.8}$$

One way of controlling the tail current to the desired value I'_{TAIL} is by changing the gate-to-source voltage of M9 with temperature. Equating (3.6) and (3.8) and solving the resulting quadratic equation for the gate-to-source voltage gives the gate-to-source voltage needed as

$$V_{GS}(T) = (V_{GS0} - V_{T0})\left(\frac{T}{T_0}\right)^{-\alpha_\mu} + V_{T0} + \alpha_v(T - T_0). \tag{3.9}$$

With M9 operating above its zero-temperature-coefficient (ZTC) point [20], the needed V_{GS} increases with temperature. A temperature-dependent voltage source can be used to approximate the relationship in (3.10). The temperature-dependent voltage source is designed in such a way that the increase in tail current compensates for the decrease in the mobility, so that the transconductance remains more constant over temperature than it would using a fixed bias voltage.

3.2 Design of all-CMOS temperature-dependent voltage source

A transistor-level circuit diagram of the proposed all-CMOS temperature-dependent voltage source is shown in Figure 3.1. The circuit consists of two transistors M10 and M11 that generate a bias voltage $V_X = 2.5\ \mathrm{V}$ and two NMOS transistors M12 and M13 that generate the temperature-dependent voltage. The circuit uses $V_{DD} = 3\ \mathrm{V}$. The circuit in Figure 3.1 is designed such that M12 operates below its ZTC point, and M13 operates above its ZTC voltage. This is accomplished by setting the bias voltage V_X above the ZTC point of M13 using diode-connected transistors M10 and M11. The difference between V_X and V_{BIAS} is set below the ZTC voltage of M12 by design of M12 and M13; that is,

$$V_{GS12} = V_X - V_{BIAS} \leq V_{ZTC}. \tag{3.10}$$

For this, the aspect ratio of M12 must be big enough or that of M13 must be small enough. Transistor M12 operates in the saturation region below its ZTC point. Transistor M13 may operate either in the saturation region or in the linear region. For a given aspect ratio of M12, M13 should be sized so that its $i_D - v_{DS}$ characteristic lies below the ZTC current of M12.

Figure 3.2 illustrates the operation of the circuit in Figure 3.1. In this circuit, $V_X =$ 2.5 V at room temperature and transistor M13 operates near the edge of saturation. The values of the output voltage V_{BIAS} at 0°C and 125°C are shown as the intersections of the characteristics of M12 and M13. As M12 is biased below its ZTC point, its operating point moves monotonically to the right with increasing temperature. Similarly, as M13 is biased above its ZTC point, its drain current decreases monotonically with temperature. The combined effect is an increase of the output voltage V_{BIAS} with temperature.

The slope of the voltage-temperature characteristic of the temperature-dependent voltage source can be made higher or lower by adjusting V_{GS12} closer to or farther from the ZTC point. If a higher change in V_{BIAS} is required, V_{GS12} is adjusted such that it is farther from the ZTC point and closer to the threshold voltage. This can be accomplished by decreasing the aspect ratio of M13 or increasing the aspect ratio of M12, which decreases V_{GS12}. The V_{GS} voltage being farther from the ZTC voltage results in a greater sensitivity of the output voltage V_{BIAS} to temperature variations and hence the higher slope of voltage-temperature characteristics. Similarly, if a smaller change in V_{BIAS} is required, the aspect ratio of M13 is made larger or the aspect ratio of M12 is made smaller, which increases V_{GS12}. This moves M12 closer to its ZTC point, reducing the sensitivity of V_{BIAS} with temperature.

The effect of V_X on the temperature coefficient of V_{BIAS} is only slight. The value of V_X can be selected to set the level of V_{BIAS} without having much effect on the temperature coefficient of V_{BIAS}. In the design process, V_X is used to adjust the level of V_{BIAS} after the temperature coefficient has been set by adjusting the aspect ratios of M12 and M13.

The variation of the output voltages of two example temperature-dependent voltage source designs, both based on Figure 3.1, are shown in Figure 3.3. Both use

$V_{DD} = 3$ V. The MOSFET channel dimensions and the nominal value of V_{BIAS} at room temperature are shown in Table 3.1. Different temperature characteristics are achieved by the two designs. The design with the largest value of $\frac{\left(\frac{W}{L}\right)_{12}}{\left(\frac{W}{L}\right)_{13}}$ yields the source having the largest temperature coefficient. Likewise, the smallest value of $\frac{\left(\frac{W}{L}\right)_{12}}{\left(\frac{W}{L}\right)_{13}}$ yields the source with the smallest temperature coefficient. Source 1 with $\frac{\left(\frac{W}{L}\right)_{12}}{\left(\frac{W}{L}\right)_{13}} = 10$, has a temperature coefficient of 1.30 mV/ºC. For Source 2, this quantity is increased to 1041, resulting in an increase in the increase in the temperature coefficient to 2.08 mV/ºC. For the designs shown, the variation in the output voltage is approximately linear with temperature between 25^{o}C and 125^{o}C.

In this method, the temperature coefficient and the voltage levels can be independently set for the temperature-dependent voltage sources. The voltage level can be set by V_X and the temperature coefficient can be set by adjusting the aspect ratio of M13. This method is used in temperature-compensating OTAs used in the design of bandpass filters and sinusoidal oscillators.

Table 3.1 Example temperature-dependent source designs

	Source 1	Source 2
W×L, M10	2 μm × 10 μm	2μm × 10 μm
W×L, M11	2 μm × 10 μm	2μm × 10 μm
W×L, M12	20 μm × 2 μm	100 μm × 0.8 μm
W×L, M13	2 μm × 2 μm	1.2 μm × 10 μm
V_X (V)	1.65	1.62
V_{BIAS} (V) at room T	0.83	1.10
TC (mV/ºC)	1.30	2.08

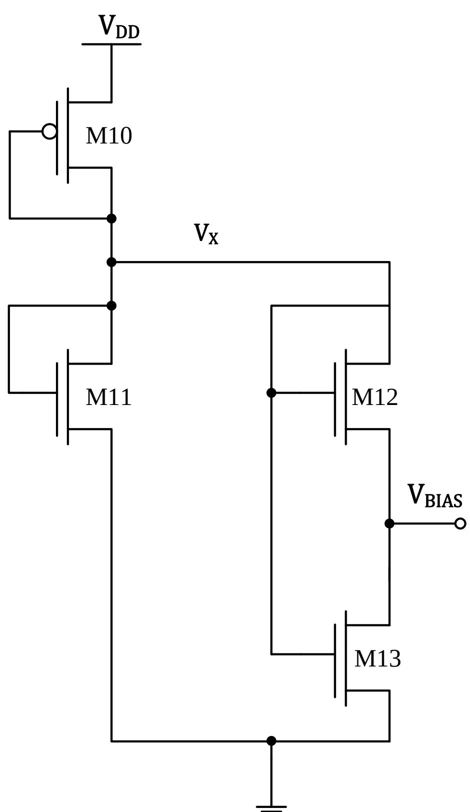

Figure 3.1 All-CMOS temperature-dependent voltage source.

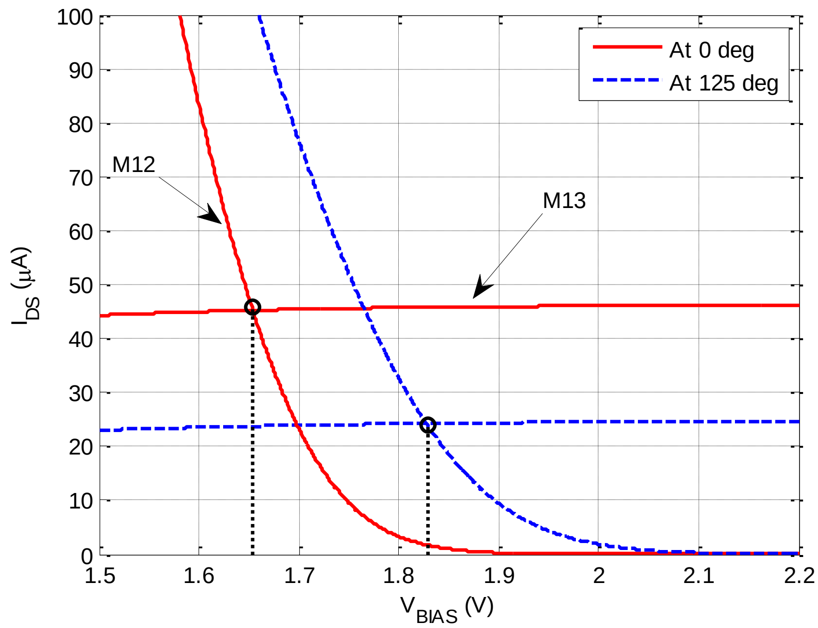

Figure 3.2 Temperature-dependent voltage source operating points at 0°C and 125°C.

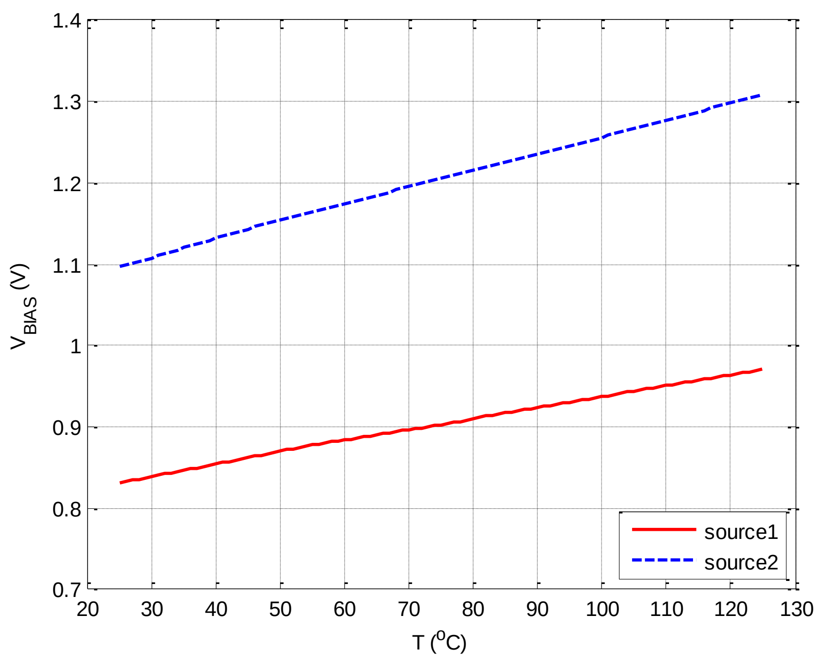

Figure 3.3 Example temperature-dependent voltage source output with temperature

3.3 Design of temperature-compensated OTA

For a given value of gate-to-source voltage of M9 at room temperature, V_{GS0}, a transconductance value g_m of an uncompensated OTA changes according to (3.7). In order to temperature-compensate the OTA, the gate-to-source voltage of M9 should be varied with temperature according to (3.9). To design the compensation, the value of V_{GS} required at the highest temperature of interest is calculated using (3.9). Thus, the necessary temperature coefficient for the temperature-dependent voltage source can be obtained as $TC = \frac{V_{GS}-V_{GS0}}{T-T_0}$. A temperature-dependent voltage source with a temperature coefficient close to the one calculated can be used to bias the tail current source, thus approximately compensating the temperature variations in the transconductance value.

An OTA is designed based on Figure 2.12 with the dimensions of the transistors M1 through M9 given in Table 3.2 and a fixed gate voltage of –1.76 V used for the tail current source M9. The OTA uses a supply voltage of ±3 V. With $V_{SS} = –3V$ as the negative supply voltage, the resulting $V_{GS0} = 1.24$ V. The g_m value of the uncompensated OTA varies significantly with temperature, from 2.50 µA/V at 25ºC to 1.80 µA/V at 125ºC.

Using (3.9), the theoretical value of V_{GS} required to compensate the OTA at 125ºC (398 K) is given by $V_{GS}(398) = 1.40$ V. Thus, the required temperature coefficient of the temperature-dependent voltage source is calculated as 1.6 mV/ºC, which is used as the starting point to compensate the OTA. A temperature-dependent voltage source with a temperature coefficient close to the calculated value is applied to the OTA. The temperature coefficient is then adjusted to get the best overall result.

In order to compensate this OTA, a nominal value of $V_{BIAS} = -1.76$ V at room temperature is used. Figure 3.4 shows the simulated temperature characteristic of this temperature-dependent voltage source. The V_{BIAS} varies from –1.76 V at 25ºC to –1.56 V at 125ºC, resulting in a slope of 2.0 mV/ºC, which is close to the theoretical approximation of 1.6 mV/ºC. Figure 3.5 shows the architecture of an OTA which uses this temperature-dependent voltage source for temperature compensation. The MOSFET channel dimensions for this OTA are shown in Table 3.2. The g_m of this OTA varies from 2.5 µA/V to 2.55 µA/V, over the temperature range from 25ºC to 125ºC, which is an improvement over the uncompensated structure. The compensated and uncompensated OTA characteristics are shown in Figure 3.6. The load assumed for the simulation was a 100-pF capacitor with a sinusoidal wave of 1MHz applied at the input of the OTA, which results in a 1.6 kΩ load impedance.

Table 3.2 Channel dimensions of transistors in a temperature-compensated OTA

Device	W × L (µm × µm)
M1, M2	1.2 × 15
M3,M4,M5,M6	150 × 5
M7,M8	30 × 5
M9	2.3 × 5
M10	1.2 × 0.5
M11	1.2 × 0.8
M12	120 × 0.8
M13	1.2 × 15

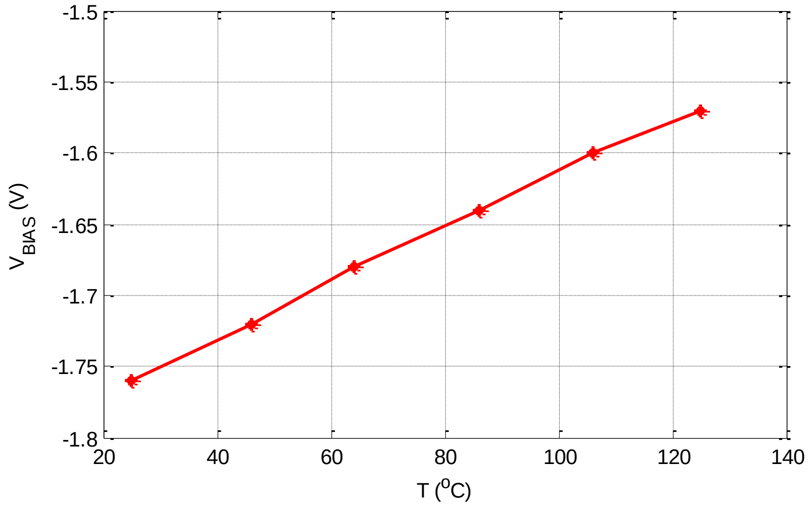

Figure 3.4 Characteristics of temperature-dependent voltage source used to compensate the OTA

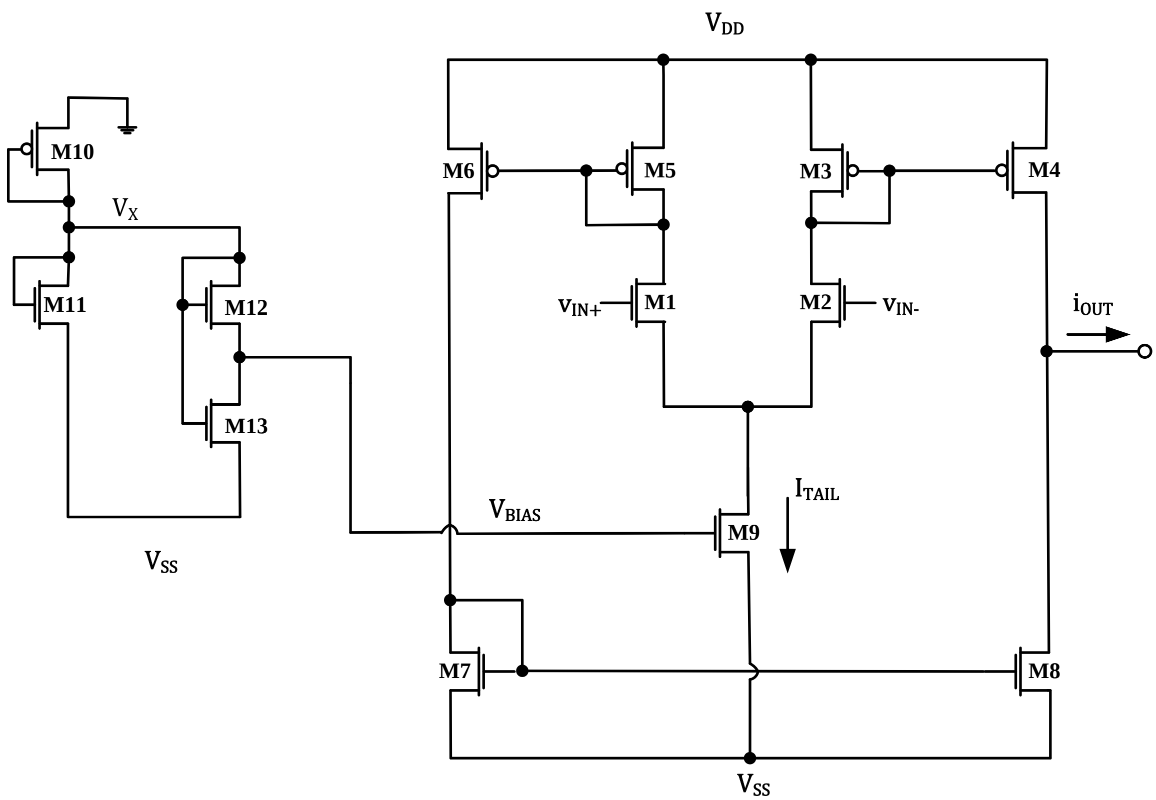

Figure 3.5 Temperature-compensated OTA

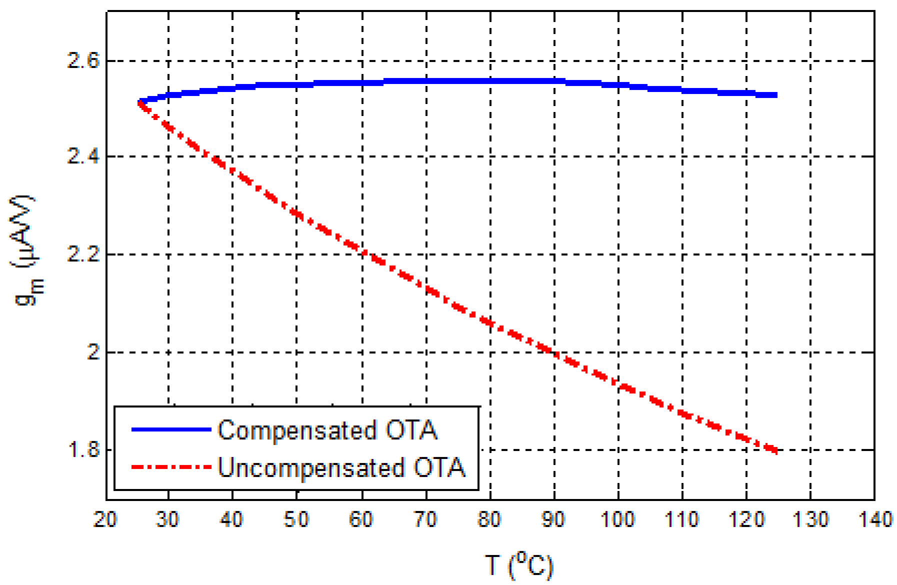

Figure 3.6 Compensated and uncompensated OTA characteristics

3.4 Summary of design procedure

The design procedure for temperature compensation of an OTA can be summarized in the following steps:

i. For an uncompensated OTA with a given nominal value of g_m determine V_{GS0}. Calculate $V_{BIAS} = V_{GS0} - V_{SS}$; this gives the voltage level of V_{BIAS} required at room temperature.

ii. With the value of V_{BIAS} and the emperical values of $\alpha_v = -2.70$ mV/ºC and $\alpha_\mu = -1.8$, estimate the required variation of V_{BIAS} over the desired temperature range using (3.9). This gives an estimate of the required temperature coefficient of V_{BIAS} for the temperature compensation.

iii. To set the voltage level of V_{BIAS} calculated from step i., first set V_X through M10 and M11. Then set V_{BIAS} through M12 and M13 and such that V_X and V_{BIAS} satisfy (3.11).

iv. Simulate the temperature characteristics of the voltage V_{BIAS} for the given temperature range. The goal is to make the temperature coefficient of V_{BIAS} as close as possible to the one calculated in step ii. For a higher change of V_{BIAS} with temperature, increase $\frac{\left(\frac{W}{L}\right)_{12}}{\left(\frac{W}{L}\right)_{13}}$. For a lower change of V_{BIAS} with temperature, decrease $\frac{\left(\frac{W}{L}\right)_{12}}{\left(\frac{W}{L}\right)_{13}}$.

v. Follow an iteration of step iv until the goal is achieved.

vi. Once the estimated TC is achieved, readjust V_{BIAS} level, if necessary, through V_X.

vii. Incorporate the voltage source in the OTA to supply the gate bias voltage of M9.

viii. Simulate the temperature characteristics of the OTA. If g_m of the OTA increases with temperature, decrease the TC of V_{BIAS}; if g_m decreases with temperature increase the TC of V_{BIAS}. Achieve the desired changes in the TC the same way as in step iv.

ix. Follow an iteration of step viii until g_m at 25ºC is equal to g_m at 125ºC.

A flowchart of the designed procedure is shown in Figure 3.7. This design algorithm is applied to temperature compensate all the OTAs used in the design of two tuned pairs of g_m-C bandpass filters and sinusoidal oscillators. The design detail and the simulation results of the tuned pairs of temperature-compensated bandpass filters and sinusoidal oscillators are shown in Chapter IV.

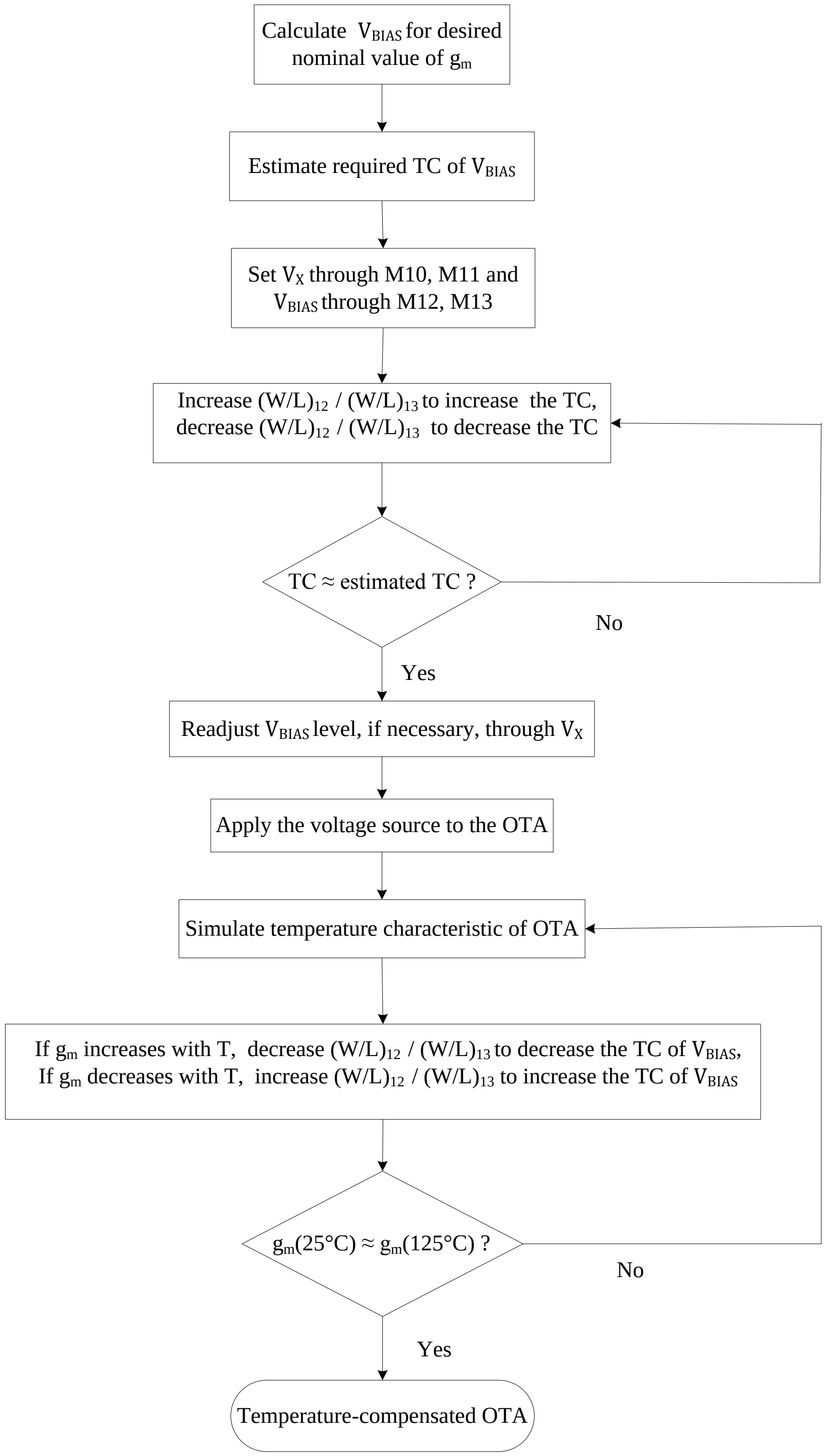

Figure 3.7 Design flow of temperature compensation of an OTA

CHAPTER IV

FREQUENCY-TUNED BANDPASS FILTER AND SINUSOIDAL OSCILLATOR

4.1 Design of tuned bandpass filter and sinusoidal oscillator

The tuned bandpass filters and sinusoidal oscillators presented in this thesis provide temperature-insensitive operation over a temperature range from 25°C to 125°C. In this section, the tuning of the center frequency of a g_m-C bandpass filter and the frequency of oscillation of a g_m-C sinusoidal oscillator is presented. Figure 4.1 shows a generalized second-order g_m-C bandpass filter with four transconductors g_{mb1}, g_{mb2}, g_{mb3} and g_{mb4} in a closed loop with capacitive loads C_{b1} and C_{b2} as discussed in Section 2.1.2(B). The center frequency of this g_m-C bandpass filter is given by

$$\omega_{b0} = \sqrt{\frac{g_{mb3}g_{mb4}}{C_{b1}C_{b2}}}. \tag{4.1}$$

Figure 4.2 shows a sinusoidal g_m-C oscillator with four transconductors g_{mQ}, g_{ms2}, g_{ms3} and g_{ms4} in a closed loop with capacitive loads C_{s1} and C_{s2} as discussed in Section 2.2.3. The frequency of oscillation of this oscillator is given by

$$\omega_{S0} = \sqrt{\frac{g_{ms3}g_{ms4}}{C_{s1}C_{s2}}}. \tag{4.2}$$

It is observed that the transconductors g_{mb3} and g_{mb4} determine the center frequency of the transfer function in the filter circuit, and the transconductors g_{ms3} and g_{ms4} determine the oscillating frequency in the oscillator circuit. These two frequencies can be tuned together if matching transconductors and capacitive loads are used with $g_{mb3} = g_{ms3}$, $g_{mb4} = g_{ms4}$, $C_{b1} = C_{s1}$, and $C_{b2} = C_{s2}$. In the filter circuit, the additional transconductors g_{mb1} and g_{mb2} determine the bandwidth and the gain of the bandpass filter; in the oscillator circuit, the additional transconductors g_{ms2} and g_{msQ} are chosen to ensure oscillation.

Non-ideal finite transconductor output resistances will affect the frequency characteristics of the circuits [8]; however, they are expected to have the same effect on the frequencies for both circuits, because the transconductors and the capacitors that determine the frequencies are exactly the same.

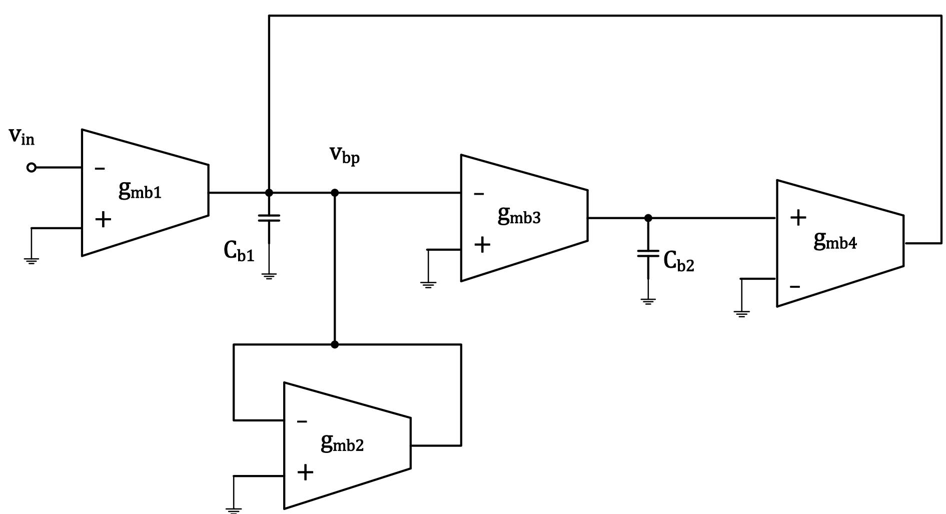

Figure 4.1 A g_m-C bandpass filter

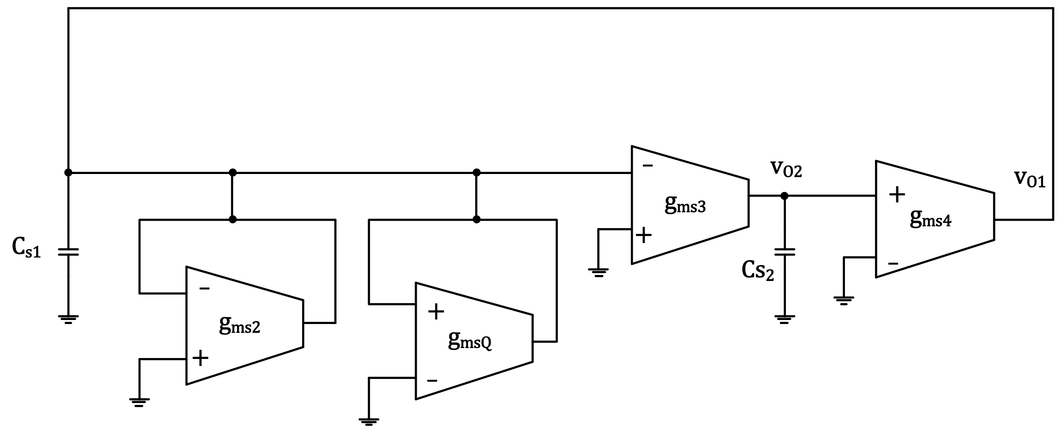

Figure 4.2 A g_m-C quadrature oscillator

The proposed temperature-insensitive tuned bandpass filter and sinusoidal oscillator designs are simulated in a 0.5-μm SOI process using a ±3 V power supply. Two different pairs of bandpass filters and sinusoidal oscillators, one tuned at 40 kHz and the other tuned at 1 MHz, are designed. The tuned pairs are simulated over a temperature range of 25°C to 125°C and over the process corners.

4.1.1 Choice of filter and oscillator parameters

The tuned pairs are designed by first selecting the nominal transconductance values of the OTAs and the capacitances of the loads. As seen from (4.1) and (4.2), a low-frequency pair can be designed with low OTA transconductance values or a high capacitance values. For these pairs, OTAs with higher transconductance values require even larger capacitors. For the 40-kHz pair, in order to ensure that value of the capacitors is not too high, the capacitance values are fixed at 10 pF. The desired frequency is then obtained using a transconductance value of 2.50 μA/V for g_{mb3}, g_{ms3}, g_{mb4} and g_{ms4}. For a g_m-C bandpass filter, the gain at the center frequency is $G = \frac{-g_{mb1}}{g_{mb2}}$ and the quality factor is $Q = \sqrt{\frac{C_{b1}}{C_{b2}}} \frac{\sqrt{g_{mb3} g_{mb4}}}{g_{mb2}}$ as shown in Section 2.1.2(B). The bandpass filter in the pair is desired to have a bandwidth of 5 kHz and a gain of 20 dB. Therefore, the g_m values of $g_{mb1} = 2.50$ μA/V and $g_{mb2} = 0.25$ μA/V are chosen. For the oscillator, g_m values of $g_{msQ} = 2.50$ μA/V and $g_{ms2} = 2.40$ μA/V, which satisfy the oscillation requirements, are chosen.

The 1-MHz pair is designed with 0.5-pF capacitors and a transconductance value of 3.70 μA/V for g_{mb3}, g_{ms3}, g_{mb4} and g_{ms4}. The bandpass filter in the pair is desired to have a bandwidth of 0.4 MHz and a gain of 8.7 dB. Therefore, the g_m values of $g_{mb1} = 3.70$ μA/V and $g_{mb2} = 1.35$ μA/V are chosen. For the oscillator, g_m values of $g_{msQ} = 3.50$ μA/V and $g_{ms2} = 3.28$ μA/V, which satisfy the oscillation requirements, are chosen. Design of the 1-MHz pair required four different OTAs to get the desired frequency characteristics of the pair. The capacitive load assumed for all nominal g_m values is 100 pF.

Tables 4.1 and 4.2 show the transconductance values of the OTAs used in the design of the bandpass filters and sinusoidal oscillators with nominal frequencies 40 kHz and 1 MHz. The OTA designed to have $g_m = 2.50$ μA/V turned out in simulation to have $g_m = 2.48$ μA/V which corresponds to an error of 1%. All of the other designs produced g_m values accurate to the given precisions. The design details are given in Section 4.1.2.

Figure 4.3 shows the ideal frequency response of a second-order bandpass filter, based on the transconductance and capacitance values in Table 4.1. The filter has a center frequency of 39.8 kHz, a bandwidth of 3.9 kHz and a gain of 20.2 dB. Figure 4.4

shows the ideal frequency response of a second-order bandpass filter, based on the transconductance and capacitance values in Table 4.2. The filter has a center frequency of 1.15 MHz, a bandwidth of 0.4 MHz and a gain of 8.7 dB. The detailed designs and the simulation results are presented and discussed next.

Table 4.1 Transconductance and capacitance values for 40-kHz bandpass filter and oscillator

Bandpass Filter ω_0=39.8 kHz, BW = 3.9 kHz, G = 20.2 dB				Oscillator ω_0=39.8 kHz, poles at 4 ± j248 ms^{-1} (0.92° with jω axis)			
OTA	g_m μA/V	Capacitor	Value pF	OTA	g_m μA/V	Capacitor	Value pF
g_{mb1}	2.48			g_{msQ}	2.48		
g_{mb2}	0.25			g_{ms2}	2.40		
g_{mb3}	2.48	C_{b2}	10	g_{ms3}	2.48	C_{s2}	10
g_{mb4}	2.48	C_{b1}	10	g_{ms4}	2.48	C_{s1}	10

Table 4.2 Transconductance and capacitance values for 1-MHz bandpass filter and oscillator

Bandpass Filter ω_0=1.15 MHz, BW =0.4 MHz, G = 8.7 dB				Oscillator ω_0=1.15 MHz, poles at 0.22 ± j7.4 μs^{-1} (1.70° with jω axis)			
OTA	g_m μA/V	Capacitor	Value pF	OTA	g_m μA/V	Capacitor	Value pF
g_{mb1}	3.70			g_{msQ}	3.50		
g_{mb2}	1.35			g_{ms2}	3.28		
g_{mb3}	3.70	C_{b2}	0.5	g_{ms3}	3.70	C_{s2}	0.5
g_{mb4}	3.70	C_{b1}	0.5	g_{ms4}	3.70	C_{s1}	0.5

4.1.2 Transistor-level OTA designs

The filter and oscillator designs require seven different OTAs. Different transconductance values are obtained by designing two OTAs at first and then modifying their designs to get the rest of the OTAs. Starting with a fixed design for the transistors M1, M2, M7 and M8 and using $\left(\frac{W}{L}\right)_{3,5} = \left(\frac{W}{L}\right)_{4,6}$, an OTA with transconductance value 3.70 μA/V and another with transconductance value 2.48 μA/V are obtained by adjusting the aspect ratio of the tail current source M9. A higher aspect ratio of M9 results in the higher transconductance value and a lower aspect ratio results in the lower transconductance value. From the two designs, the remaining designs are made by varying $\left(\frac{W}{L}\right)_{4,6}$ relative to $\left(\frac{W}{L}\right)_{3,5}$. Within a family, $\left(\frac{W}{L}\right)_{3,5}$ does not vary. The value of $\left(\frac{W}{L}\right)_{3,5}$ is made large so that the current mirror ratios may be varied with a high degree of resolution. By doing this, accurate transconductance values can be obtained more conveniently by modifying the 3.70-μA/V and the 2.48-μA/V designs. Table 4.3 shows the MOSFET channel dimensions for the transistors used in the design of the OTAs.

The OTAs with transconductance values 0.25 μA/V and 2.40 μA/V are obtained by adjusting the current-mirror ratios of M3-M4 and M5-M6 in the 2.48-μA/V OTA design. The OTA with the transconductance value of 0.25 μA/V is obtained by making the current mirrors M3-M4 and M5-M6 with ratio 10:1 whereas the original 2.48 μA/V design uses a ratio of 1:1. This results in approximately one tenth of the output current supplied to the load, decreasing the overall transconductance value by a factor slightly lower than 10 giving a value of 0.25 μA/V from 2.48 μA/V. Similarly, the OTAs with transconductance values 3.50 μA/V, 3.28 μA/V and 1.35 μA/V are obtained by adjusting the aspect ratio of the current mirrors M3-M4 and M5-M6 in the 3.70 μA/V-OTA design.

The uncompensated OTAs are designed by applying an ideal voltage V_{BIAS} to the gate of M9. Temperature compensation of the OTA with transconductance value 2.48 μA/V is achieved by replacing the ideal voltage V_{BIAS} with the temperature-dependent voltage source designed and simulated in Section 3.3. Temperature compensation of the OTAs with transconductance values 0.25 μA/V and 2.48 μA/V is achieved by following step viii in Section 3.4 and by adjusting the TC of the temperature-dependent voltage source used for the 2.48 μA/V-OTA to get the best overall result. Similarly, the temperature compensation of the OTA with transconductance value 3.70 μA/V is achieved by using a temperature-dependent voltage source with a TC of 1.8 mV/ºC. Temperature compensation of the OTAs with the transconductance values 3.50 μA/V, 3.28 μA/V and 1.35 μA/V is achieved by adjusting the TC of the temperature-dependent voltage source used for the 3.70 μA/V-OTA to get the best overall result.

As the 40-kHz bandpass filter design requires a 10-pF capacitor, it would occupy a large area on a chip. This filter is first designed and simulated using an ideal capacitor. Then, it is simulated using the capacitance obtained from the capacitor-multiplier circuit design given in Section 2.5.

The simulation results for the various bandpass filter and sinusoidal oscillator designs are presented in the next section.

Table 4.3 MOSFET channel dimensions for temperature-compensated OTAs

	MOSFET Channel Dimensions W × L (µm × µm)								
g_m value µA/V	OTA					Temperature compensation			
	M1, M2	M3,M5	M4,M6	M7, M8	M9	M10	M11	M12	M13
3.7	1.2 × 15	300 × 5	300 × 5	30 × 5	4.5 × 10	1.2 × 0.5	1.2 × 0.8	120 × 0.8	1.5 × 14
3.5	1.2 × 15	300 × 5	280 × 5	30 × 5	4.5 × 10	1.2 × 0.5	1.2 × 0.8	120 × 0.8	1.5 × 14
3.28	1.2 × 15	300 × 5	266 × 5	30 × 5	4.5 × 10	1.2 × 0.5	1.2 × 0.8	120 × 0.8	1.5 × 14.3
1.35	1.2 × 15	300 × 5	115× 5	30 × 5	4.5 × 10	6.0 × 2.0	6.0 × 2.4	200 × 1.4	1.5 × 14.4
2.48	1.2 × 15	150 × 5	150 × 5	30 × 5	2.3 × 10	1.2 × 5.0	1.2 × 0.8	120 × 0.8	1.2 × 15
2.40	1.2 × 15	150 × 5	143 × 5	30 × 5	2.3 × 10	1.2 × 5.0	1.2 × 0.8	120 × 1.0	1.2 × 15
0.25	1.2 × 15	150 × 5	15 × 5	30 × 5	2.3 × 10	1.2 × 5.0	1.2 × 0.8	120 × 0.8	1.2 × 14.8

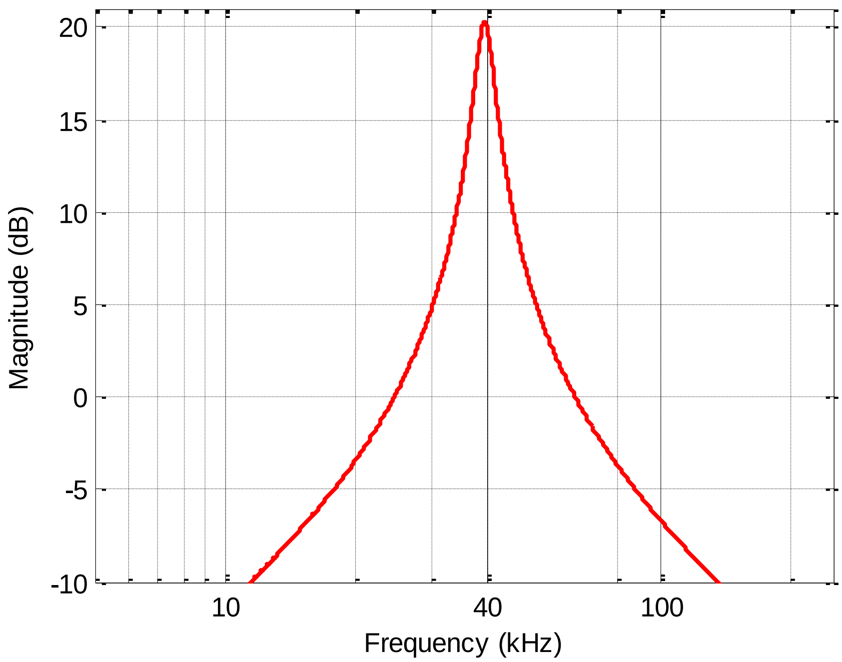

Figure 4.3 Ideal frequency response of a 40-kHz bandpass filter

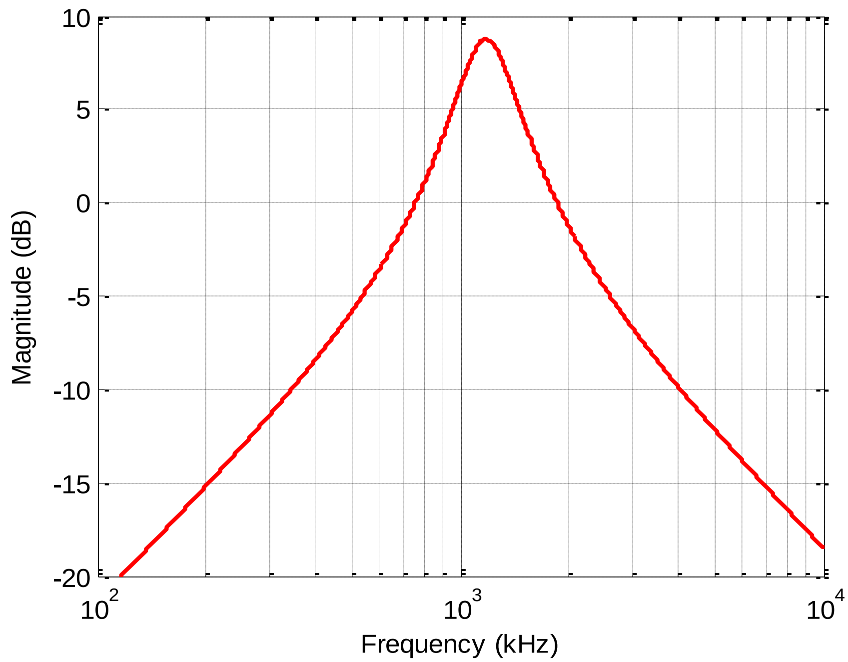

Figure 4.4 Ideal frequency response of a 1-MHz bandpass filter

4.2 Simulation of bandpass filter and sinusoidal oscillator with temperature

The bandpass filters and sinusoidal oscillators are simulated using the temperature-compensated OTAs designed in Section 4.1.2. The transistor-level design and simulation of the proposed circuits have been carried out using the Cadence® ICFB design environment. The transistor-level schematics and their simulations have been carried out using Schematic Editor and Virtuoso® Spectre® Circuit Simulator, respectively. The simulation results for the temperature-compensated bandpass filters and sinusoidal oscillators over a temperature range of 25°C to 125°C are shown in following sub-sections.

4.2.1 Simulation of bandpass filters

The bandpass filters are simulated using the circuit setups described in Section 4.1 and shown in Figure 4.1 with ideal capacitors connected as loads to the transconductors. Both bandpass filters are supplied with a sinusoidal input of 5 mV peak amplitude.

Figure 4.5 shows the simulated frequency response of an uncompensated 40-kHz bandpass filter for the temperatures 25°C and 125°C. The simulation results for the uncompensated filter are shown only at 25°C and 125°C because the filter properties are observed to change monotonically from 25°C to 125°C. At 25°C, the bandpass filter is similar to the ideal frequency response, shown in Figure 4.3. The center frequency of the bandpass filter is 40.2 kHz, which is a difference of 0.4 kHz, or 1%, from the nominal value of 39.8 kHz. The bandwidth is 5.05 kHz and the gain is 19.0 dB, which are variations of 22% and 9.5%, respectively, from the nominal values of 3.90 kHz and 20.2 dB. At 125°C, the center frequency of the bandpass filter is observed to have decreased from 40.2 kHz to 27.0 kHz, which is a variation of 28% over this temperature range. The bandwidth changes from 5.05 kHz at room temperature to 5.40 kHz at 125°C and the gain changes from 19.0 dB at room temperature to 16.0 dB at 125°C, which are variations of 8% and 15%, respectively.

Figure 4.6 shows the frequency response of the temperature-compensated 40-kHz bandpass filter simulated at 25°C, 85°C and 125°C. The simulation at 85°C is done because the maximum transconductance values for the different OTAs are observed at 85°C or a temperature very close to it, as seen in Figure 3.6. The center frequency of this filter is observed to be farthest from its room-temperature value at 85°C; at that temperature, the center frequency is 42.45 kHz, which is a variation of 2.25 kHz, or 5.6%, from the room-temperature value of 40.20 kHz. The bandwidth and gain at 85°C are 5.02 kHz and 18.1 dB, which are variations of 1% and 6%, respectively, from the room-temperature values of 5.05 kHz and 19.0 dB.

Figure 4.7 shows the simulated frequency response of an uncompensated 1-MHz bandpass filter for the temperatures 25°C and 125°C. At 25°C, the center frequency, bandwidth and the gain of this filter are different from those for filters using ideal OTAs, shown in Figure 4.4. The high impedance presented by the 0.5-pF capacitor connected as load to the OTAs decreases their effective g_m values. The center frequency of the bandpass filter is 0.98 MHz, which is a difference of 0.17 MHz, or 17.3%, from the nominal value of 1.15 MHz. The bandwidth is 0.3 MHz and gain is 7.9 dB, which are variations of 25% and 9.2%, respectively, from the nominal values of 0.4 MHz and 8.7 dB. At 125°C, the center frequency of this uncompensated filter is observed to have decreased from 0.98 MHz to 650 kHz, which is a variation of 35%. The bandwidth changes from 0.3 MHz at room temperature to 0.4 MHz at 125°C and the gain changes from 7.9 dB at room temperature to 7.6 dB at 125°C, which are variations of 25% and 4%, respectively.

Figure 4.8 shows the frequency response of the temperature-compensated 1-MHz bandpass filter simulated at 25°C, 85°C and 125°C. The center frequency of this filter is observed to be farthest from its room-temperature value at 125°C; at that temperature, the center frequency is 0.94 MHz, which is a variation of 0.04 MHz, or 4.1%, from the room-temperature value of 0.98 MHz. The bandwidth and gain at 125°C are 0.35 MHz and 5.1 dB, which are variations of 13% and 35%, respectively, from the room-temperature values of 0.40 MHz and 7.9 dB. Table 4.4 shows the frequencies, gains and bandwidths for the uncompensated bandpass filters at 25°C and 125°C. Table 4.5 shows the same for the temperature-compensated bandpass filters at 25°C, 85°C and 125°C.

4.2.2 Simulation of sinusoidal oscillators

The sinusoidal oscillators are simulated using the circuit setups described in Section 4.1 and shown in Figure 4.2. The frequency spectrum of the 40-kHz sinusoidal oscillator is calculated using 7001 samples with a sampling period of 100 ns. The frequency spectrum of the 1-MHz sinusoidal oscillator is calculated using 7001 samples with a sampling period of 10 ns. The frequency spectra are then normalized by the peak value of the output waveform at room temperature. The uncompensated sinusoidal oscillator sometimes did not satisfy the requirements for oscillation for temperatures other than room temperature. Therefore, the uncompensated oscillators cannot be guaranteed to oscillate. Therefore, simulation results over 25°C to 125°C are given only for the oscillators constructed with temperature-compensated OTAs.

Figure 4.9 and Figure 4.10 show the time-domain output and the frequency spectrum of the 40-kHz sinusoidal oscillator simulated at 25°C, 85°C and 125°C. Figure 4.11 shows the frequency spectrum of a 40-kHz pure sinusoid produced with the same sampling for the sake of comparison. At 25°C, the frequency of oscillation is 40.00 kHz which is a difference of 0.02 kHz, or 0.5%, from the nominal value of 39.80 kHz. The range in the frequency of oscillation for this oscillator is observed from 40.00 kHz at 25°C to 42.85 kHz at 85°C, which is a variation of 6.6%. The amplitude of the output is observed to decrease with temperature. This is because as the temperature increases, the transistors in the current mirrors of the OTAs allow less output swing before they enter a non-linear regime of operation.

Figure 4.12 and Figure 4.13 show the time-domain output and the frequency spectrum of the 1-MHz sinusoidal oscillator simulated at 25°C, 85°C and 125°C. Figure 4.14 shows the frequency spectrum of a 1-MHz pure sinusoid produced with the same sampling for the sake of comparison. At 25°C, the frequency of oscillation is 0.99 MHz which is a difference of 0.16 MHz, or 16.2 %, from the nominal value of 1.15 MHz. The range in the frequency of oscillation for this oscillator is observed from 0.99 MHz at 25°C to 1.04 MHz at 85°C, which is a variation of 6.1%.

The difference in the characteristics of the two oscillators can be explained by considering the choices of g_{mQ} and g_{m2}. The two OTA values are used to satisfy requirements for oscillation. The difference between the two OTA values determines the accuracy of the output frequency as well as the amplitude and the distortion of the output waveform. The difference between g_{mQ} and g_{m2} in the 1-MHz oscillator is 0.22 μA/V and that in the 40-kHz oscillator is 0.08 μA/V. For the 40-kHz oscillator, the small difference between the two transconductances results in a more accurate output frequency and a less non-linear output with negligible distortion. However, the smaller difference also causes the oscillator poles to be closer to the jω axis, resulting in a small amplitude of 10 mV in the output. For the 1-MHz oscillator, the larger difference between the two transconductances results in a less accurate output frequency and a more non-linear output, resulting in some distortion in the output signal. The larger difference between the two transconductances causes its poles to be farther from the jω axis, resulting in larger amplitude of 1.8 V in the output.

Distortion in the 1-MHz oscillator output was measured using total harmonic distortion (THD), which is the ratio of the sum of the powers of all harmonic components to the power of the fundamental frequency, as given by $\mathrm{THD} = \frac{\sqrt{v_1{}^2+v_2{}^2+v_3{}^2 \ldots v_n{}^2}}{v_0{}^2}$, where v_1.. v_n, are rms values of the first n harmonics and v_0 is the rms value of the fundamental frequency. The rms value is calculated by $v_{rms} = \frac{a}{\sqrt{2}}$, where a is the amplitude of the harmonic, seen as the local peak value in the frequency spectrum plot. The THD is estimated using the first three harmonics for the 1-MHz oscillator. For the 40-kHz sinusoidal oscillator, the THD observed was negligible and was not calculated. Table 4.6 shows the changes in frequency of oscillation for both sinusoidal oscillators along with the THD for the 1-MHz sinusoidal oscillator for the given temperatures.

4.2.3 Frequency mismatch of tuned pairs

The center frequency of the bandpass filter and the frequency of oscillation of the sinusoidal oscillator vary slightly with temperature. As a result, when they are used as a pair, operating at a same temperature or at different temperatures, there can be a slight mismatch in their frequencies. When the pair is used in applications such as the one explained in Section 1.1 and shown in Figure 1.1, the center frequencies of the bandpass filters are slightly different from the modulation frequencies. This causes the signals to be attenuated at the bandpass filter outputs. For the 40-kHz pair, both operating at the same temperature, the worst-case signal attenuation is 1.5 dB, at 85°C. For the bandpass filter and the sinusoidal oscillator in a pair operating at different temperatures, the worst-case signal attenuation is 4.0 dB, which occurs for the bandpass filter operating at 25°C and the sinusoidal oscillator operating at 85°C. Similarly, for the 1-MHz pair, both operating at the same temperature, the worst-case signal attenuation is 0.9 dB, which occurs at 85°C. For the bandpass filter and the sinusoidal oscillator in a pair operating at different temperatures, the worst-case signal attenuation is 2.0 dB, which occurs for the bandpass filter operating at 85°C and the sinusoidal oscillator operating at 125°C.

The tuned pairs of bandpass filter and sinusoidal oscillator of frequencies 40-kHz and 1-MHz are designed and simulated. The temperature-sensitivity of the tuned pairs is minimal. The pairs are observed to remain tuned within 6% of each other over a temperature range of 25°C to 125°C. The worst-case signal attenuation due to mismatch of frequencies over temperature is observed to be 4.0 dB.

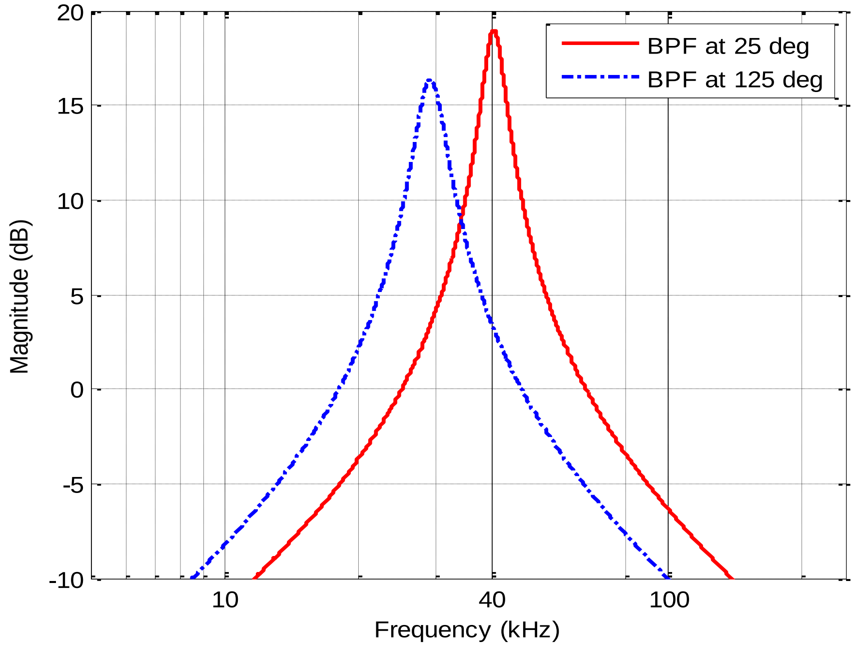

Figure 4.5 Frequency response of uncompensated 40-kHz bandpass filter

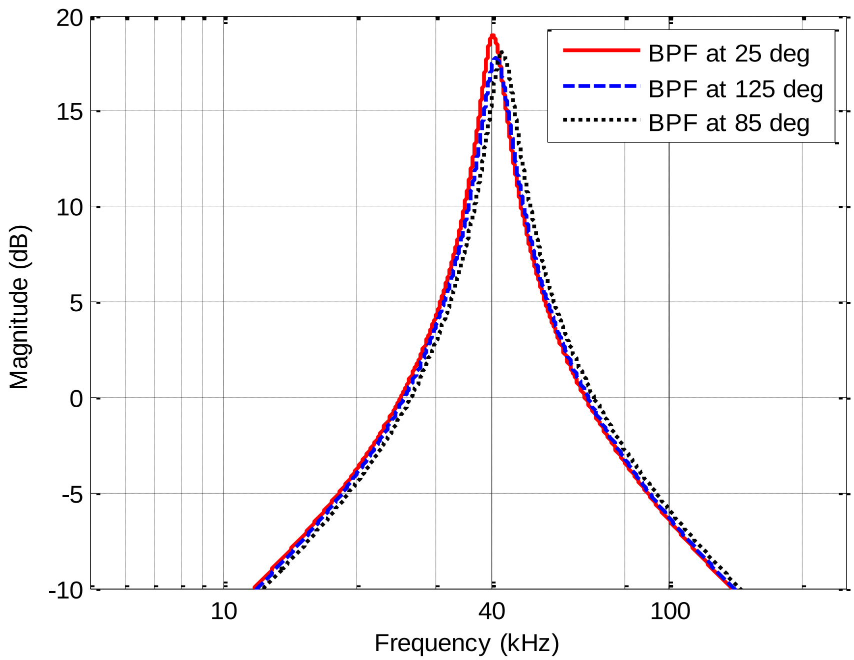

Figure 4.6 Frequency response of temperature-compensated 40-kHz bandpass filter

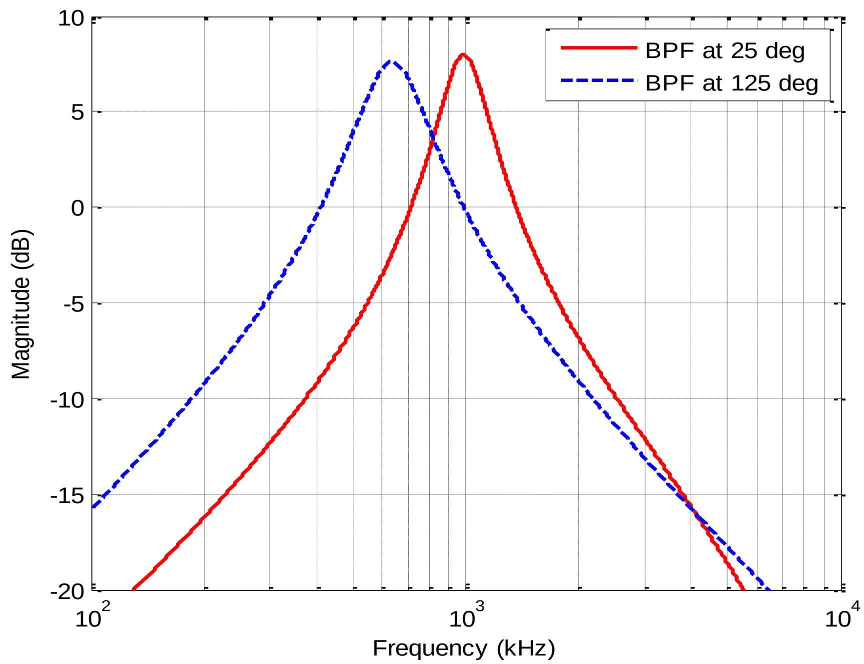

Figure 4.7 Frequency response of uncompensated 1-MHz bandpass filter

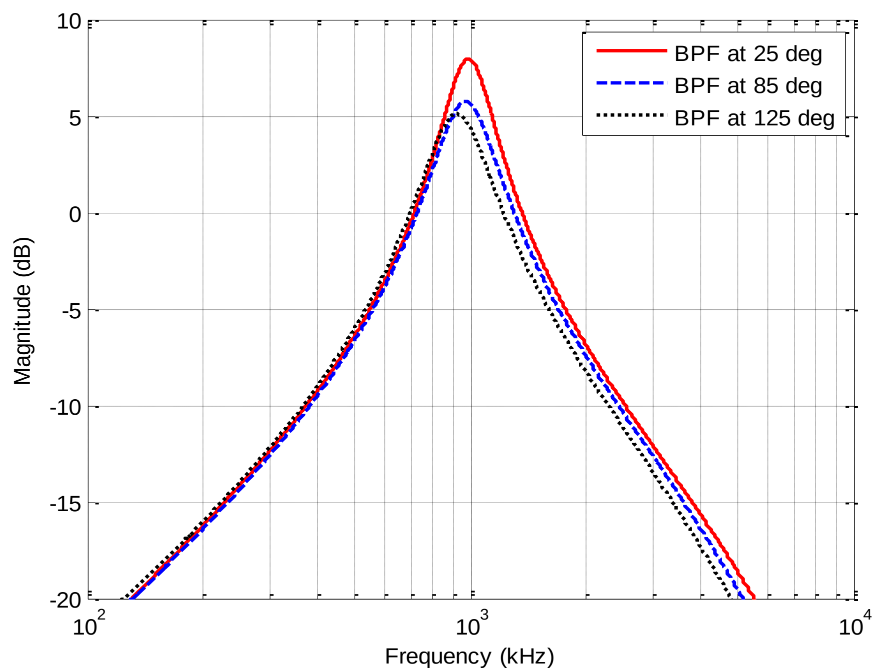

Figure 4.8 Frequency response of temperature-compensated 1-MHz bandpass filter

Table 4.4 Uncompensated bandpass filter properties at different temperatures

		25°C	125°C	Ideal
40-KHz BPF	Frequency (kHz)	40.2	27.0	39.8
	Bandwidth (kHz)	5.05	5.40	3.90
	Gain (dB)	19.0	16.0	20.2
1-MHz BPF	Frequency (MHz)	0.98	0.65	1.15
	Bandwidth (MHz)	0.3	0.4	0.4
	Gain (dB)	7.9	7.6	8.7

Table 4.5 Temperature-compensated bandpass filter properties at different temperatures

		25°C	85°C	125°C	Ideal
40-KHz BPF	Frequency (kHz)	40.20	42.45	40.85	39.80
	Bandwidth (kHz)	5.05	5.02	5.00	3.90
	Gain (dB)	19.00	18.10	17.80	20.20
1-MHz BPF	Frequency (MHz)	0.98	0.99	0.94	1.15
	Bandwidth (MHz)	0.30	0.34	0.35	0.40
	Gain (dB)	7.9	5.8	5.1	8.7

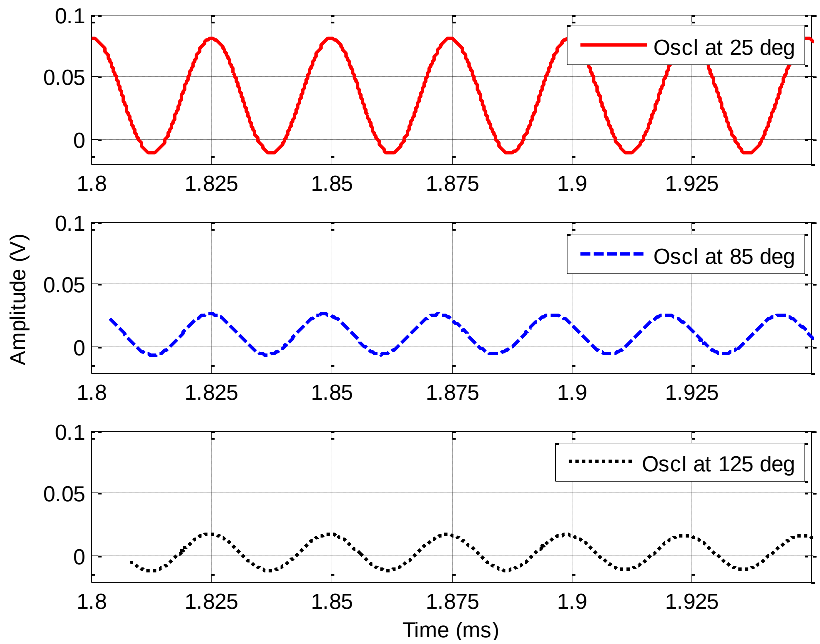

Figure 4.9 Time-domain output of a temperature-compensated 40-kHz sinusoidal oscillator

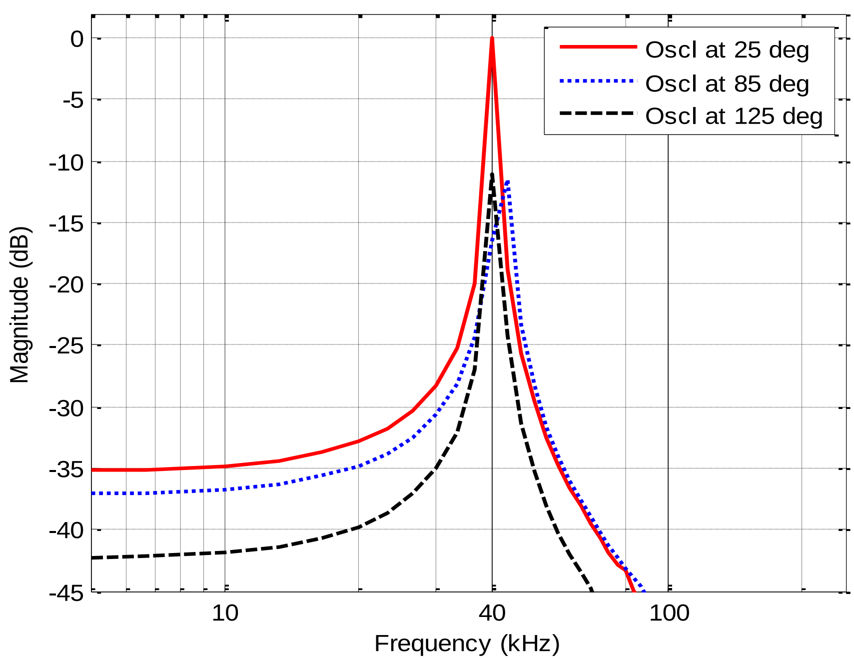

Figure 4.10 Frequency spectrum of a temperature-compensated 40-kHz sinusoidal oscillator

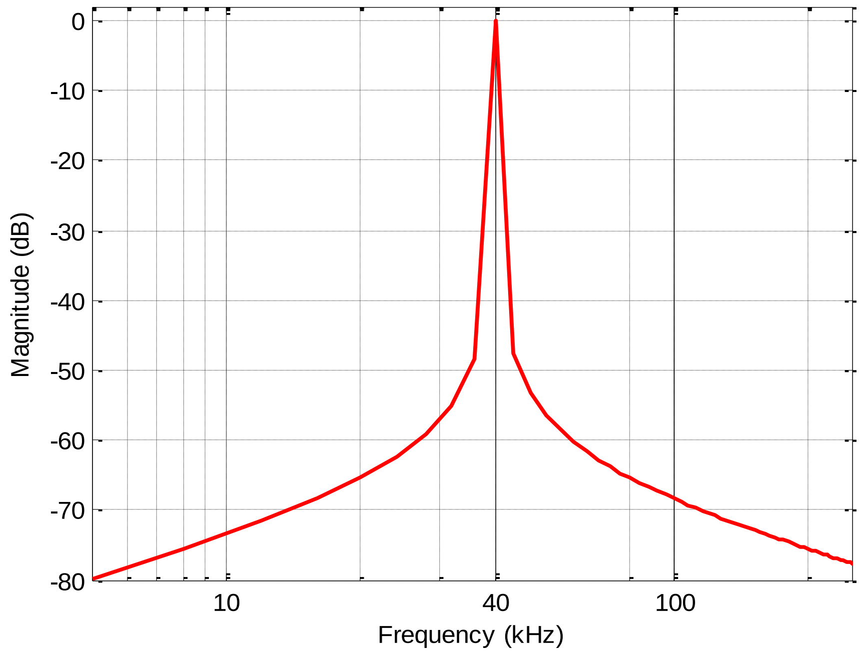

Figure 4.11 Ideal frequency spectrum of a 40-kHz sinusoidal oscillator

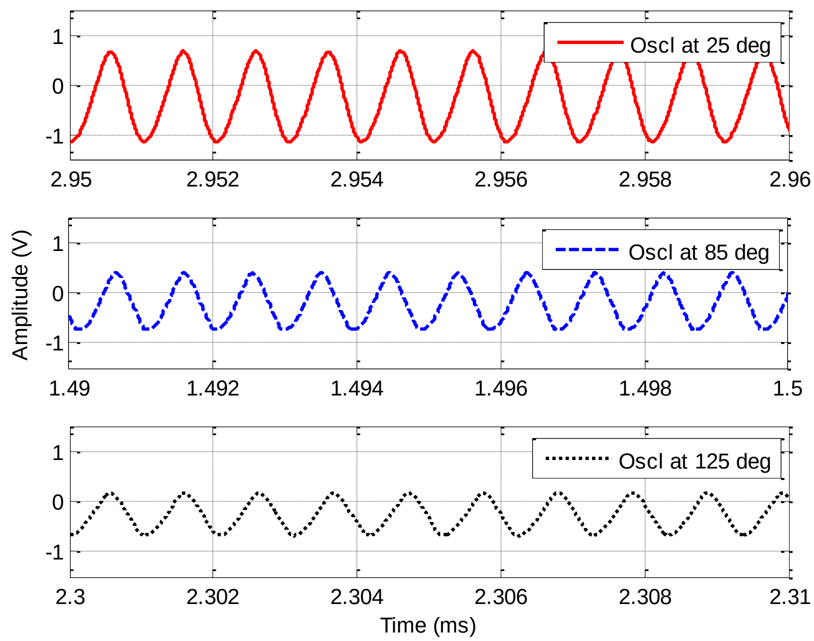

Figure 4.12 Time-domain output of temperature-compensated 1-MHz sinusoidal oscillator

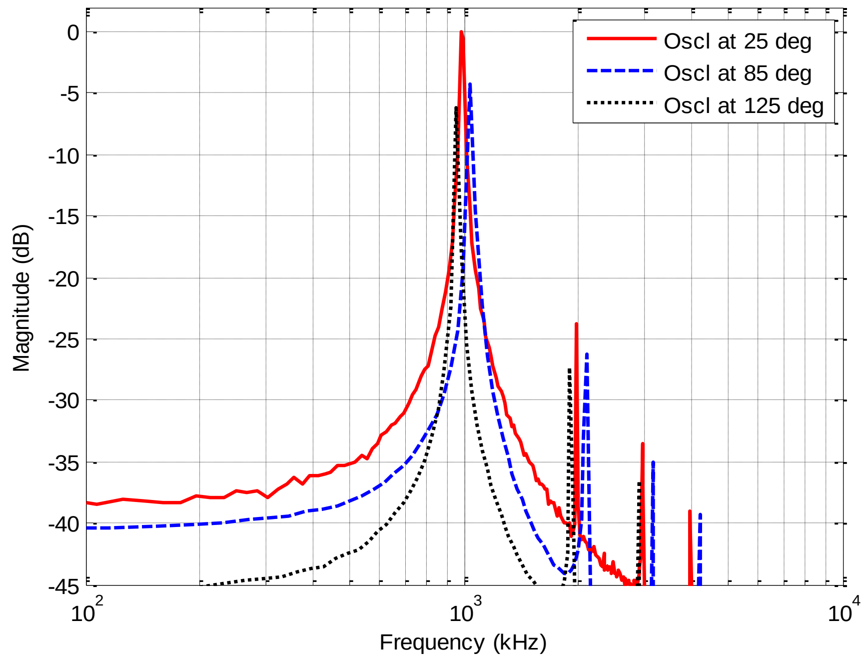

Figure 4.13 Frequency spectrum of temperature-compensated 1-MHz sinusoidal oscillator

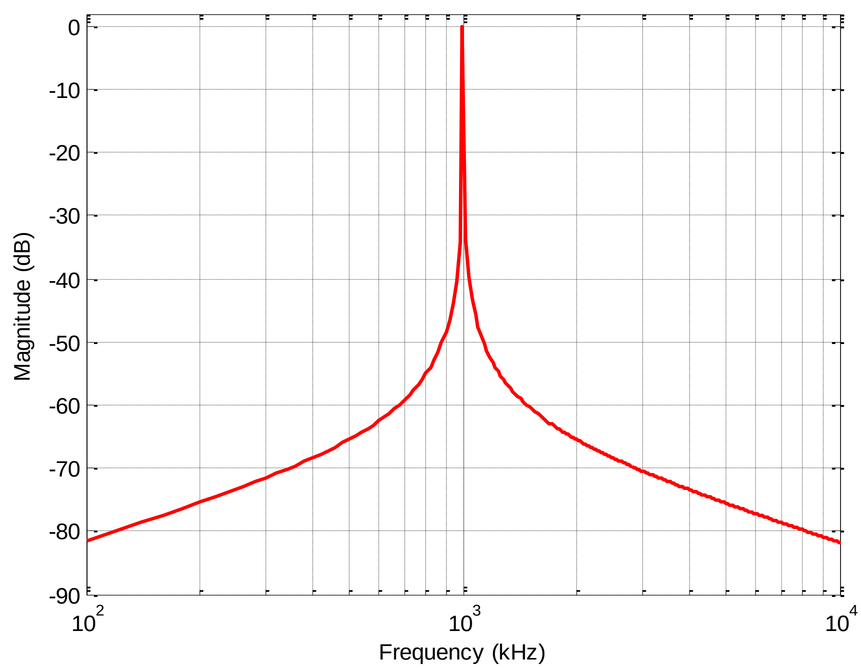

Figure 4.14 Ideal frequency spectrum of a 1-MHz sinusoidal oscillator

Table 4.6 Temperature-compensated sinusoidal oscillator frequencies at different temperatures

		25°C	85°C	125°C
40-kHz Oscillator	Frequency (kHz)	40.00	42.85	39.90
1-MHz Oscillator	Frequency (MHz)	0.99	1.04	0.95
	THD (%)	7.78	11.20	15.60

4.3 Simulation using capacitor-multiplier circuit

Circuits requiring a high value of capacitance require a large area on an integrated circuit. The design of a low-frequency filter or oscillator using the g_m-C technique often requires a high value of capacitance. With a capacitor-multiplier circuit, low-frequency circuits can be designed using smaller values of capacitance. The 40-kHz circuits designed in Section 4.1 need two 10-pF capacitors. A 10-pF capacitor requires a large area on an integrated circuit. The use of a capacitor-multiplier circuit is advantageous for the design of the 40-kHz filter. The 1-MHz circuits need two 0.5-pF capacitors. A 0.5-pF capacitor is small and does not require a large area on an integrated circuit. This makes the use of capacitor-multiplier circuit in 1-MHz filter less advantageous. Therefore, the simulation with a capacitor-multiplier circuit has been carried out for only the 40-kHz bandpass filter.

A circuit that multiplies a 1-pF capacitor 10 times to get a 10-pF capacitor is described in Section 2.5. This circuit is connected as load to the OTAs in the temperature-compensated 40-kHz bandpass filter. Figure 4.15 shows the frequency response of the 40-kHz bandpass filter designed using the transconductance values in Table 4.1 and using the capacitor-multiplier circuit as load. The center frequency of this filter is 39.4 kHz compared to 40.2 kHz for the filter using an ideal capacitor. The filter has a lower gain and a higher bandwidth than the filter using an ideal capacitor. The gain is decreased by 12.0 dB and the bandwidth is increased by 1.9 kHz. This is caused by the effective increase in the transconductance value of g_{m2} in the presence of the capacitor-multiplier circuit. The capacitor-multiplier circuit is in parallel with g_{m2} which acts as a resistor, as shown in Figure 2.7. The equivalent parallel resistance R_P of the capacitor-multiplier circuit and g_{m2} effectively decreases the equivalent resistance of $g_{mb2;}$ thus increasing its transconductance value. The increase in g_{m2} decreases the gain and increases the bandwidth of the bandpass filter as shown in Section 2.1.2(B).

The center frequency of this filter is farthest from its room-temperature value at 85°C; at that temperature, the center frequency is 42.3 kHz, which is a variation of 2.9 kHz, or 5%, from the room-temperature value of 39.4 kHz. This is similar to the 5% variation of the filter using an ideal capacitor. The bandwidth and gain at 85°C are 20.0 kHz and 5.78 dB, which are variations of 10% and 24%, respectively, from the room-temperature values of 18.1 kHz and 6.94 dB. Table 4.7 shows the bandpass filter properties for the given temperatures.

The oscillator circuit using capacitor-multiplier circuits did not always sustain an oscillation; this is due to the non-capacitive characteristics of the capacitor-multiplier at lower and higher frequencies. Therefore, the oscillator circuit with capacitor-multiplier circuits has not been implemented.

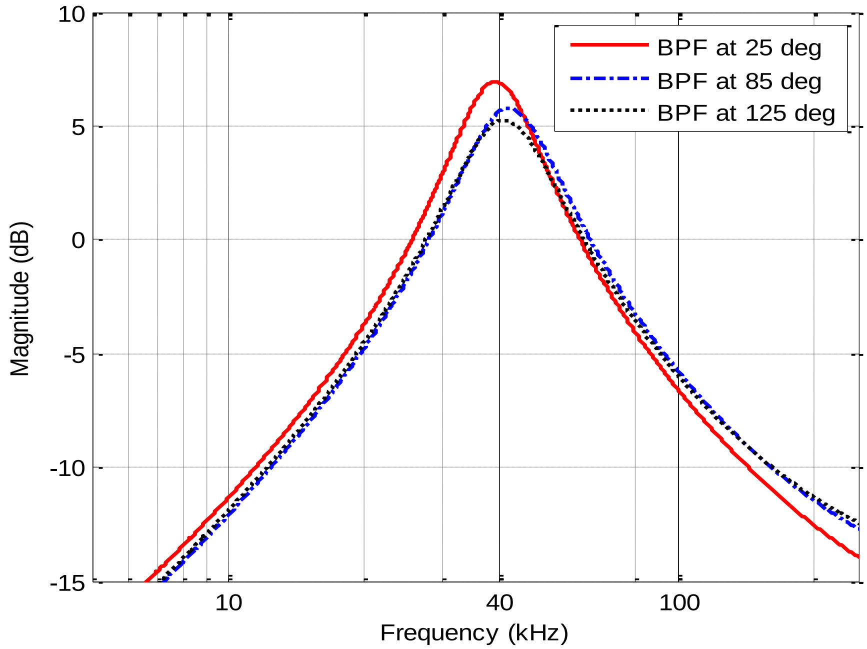

Figure 4.15 Frequency response of 40-kHz bandpass filter using capacitor-multiplier circuit

Table 4.7 Bandpass filter properties using capacitor-multiplier circuit

		25°C	85°C	125°C
40-KHz BPF	Frequency (kHz)	39.4	42.3	41.3
	Bandwidth (kHz)	18.1	20.0	19.6
	Gain (dB)	6.94	5.78	5.23

4.4 Process corner simulations

Process variations change the transconductance value of an OTA. Frequency characteristics of bandpass filters and oscillators built using OTAs are expected to change due to process variations. The pairs of bandpass filters and oscillators, tuned at frequencies 40 kHz and 1 MHz, are simulated at process corners. The simulations were carried out at room temperature for a typical-typical (TT) model and the two worst process corners, slow-slow (SS) and fast-fast (FF), where SS and FF models represent 3-σ variations.

Figure 4.16 and Figure 4.17 show the simulation results for the two bandpass filters, for the TT model and the two corners. Figure 4.18 and 4.19 show the time-domain output and the frequency spectrum of the 40-kHz sinusoidal oscillator. Figure 4.20 and Figure 4.21 show the same for the 1-MHz sinusoidal oscillator. Table 4.8 and Table 4.9 show the filter and oscillator properties, respectively, for the same three process conditions. It is observed that the process variations change the frequency characteristics of the circuits considerably. However, the oscillator frequencies are observed to move in the same direction as the bandpass filter center frequencies. At room temperature, the 40-kHz oscillator frequency remains within 1.50 kHz, or 2.5%, of the nominal bandpass filter center frequency for the SS process corner, and within 3.18 kHz, or 6%, for the FF process corner. Similarly, at room temperature, the 1-MHz oscillator frequency remains within 0.03 MHz, or 4%, of the nominal bandpass filter center frequency for the SS process corner, and within 0.10 MHz, or 7%, for the FF process corner.

In order to view how well matched the pairs stay for the three process conditions, the sinusoidal oscillator frequencies are marked on the bandpass filter frequency-response plots for each pair. Figure 4.22 and Figure 4.23 show the plots for the 40-kHz pair and the 1-MHz pair, respectively, for the three process conditions. The oscillator frequencies are marked with circles which indicate the attenuation levels for the pairs. For the 40-kHz bandpass filter, the frequency mismatch at the FF process corner is 3.18 kHz. This mismatch causes the filter output signal amplitude to be attenuated by 2.0 dB relative to the maximum gain of the filter at the FF process corner. The frequency mismatch at the SS process corner is 1.50 kHz, which causes the filter output signal amplitude to be attenuated by 3.3 dB relative to the maximum gain of the filter at the SS process corner. Similarly, for the 1-MHz pair, there is a 100-kHz mismatch at the FF process corner, resulting in an output signal attenuation of 1.6 dB. There is a 30-kHz mismatch at the SS process corner, resulting in an output signal attenuation of 1.0 dB.

A matched oscillator-filter pair may be used in an application such as the one explained in Section 1.1 and shown in Figure 1.1. In order to guarantee that the interference from a neighboring channel with the same quality factor and the same effects from process variations is at least 15.0 dB below the desired signal, the closest channel from the 40-kHz channel should be separated by at least 30 kHz. Likewise, the closest channel from the 1-MHz channel should be separated by at least 1.4 MHz. With the maximum 3.3 dB attenuation due to mismatch, the interference from the neighboring channel for both 40-kHz and 1-MHz channels will still be at least 11.0 dB below the desired signal.

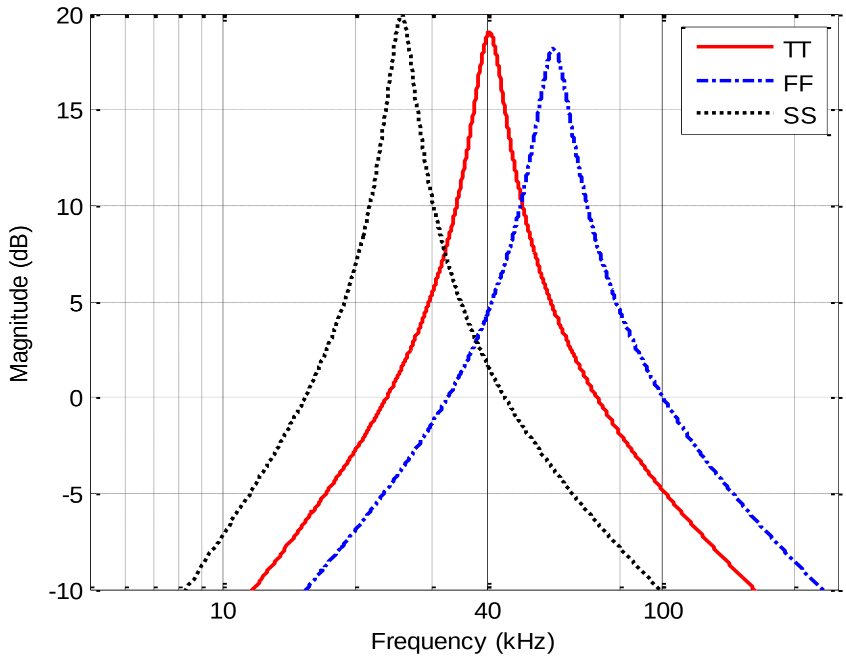

Figure 4.16 Frequency response of 40-kHz bandpass filter at process corners

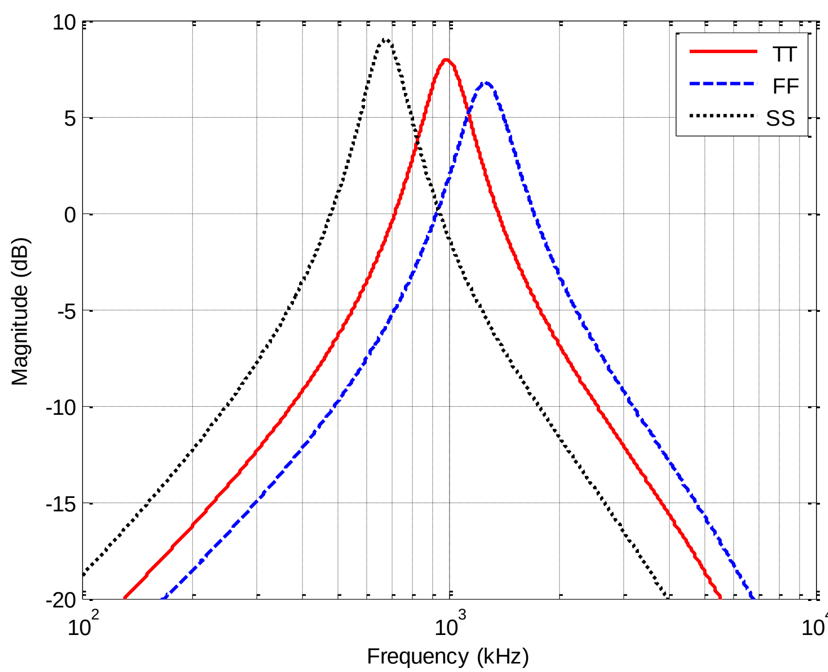

Figure 4.17 Frequency response of 1-MHz bandpass filter at process corners

Table 4.8 Bandpass filter properties at different process corners

		TT	FF	SS
40-KHz BPF	Frequency (kHz)	40.20	56.18	25.90
	Bandwidth (kHz)	5.05	7.70	3.20
	Gain (dB)	19.0	18.0	25.2
1-MHz BPF	Frequency (MHz)	0.98	1.25	0.70
	Bandwidth MHz)	0.30	0.40	0.18
	Gain (dB)	7.9	6.7	8.9

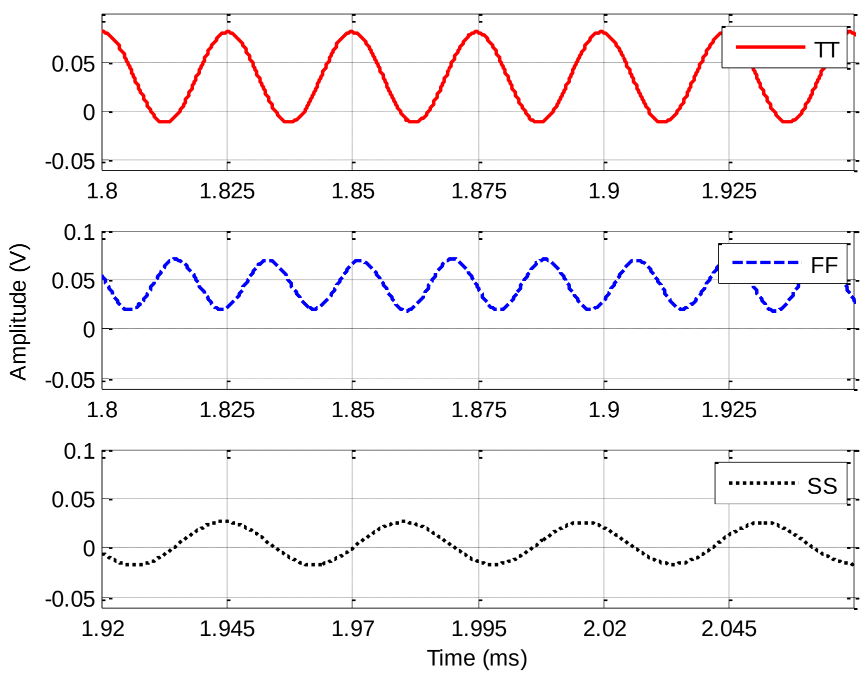

Figure 4.18 Time-domain output of 40-kHz oscillator at process corners

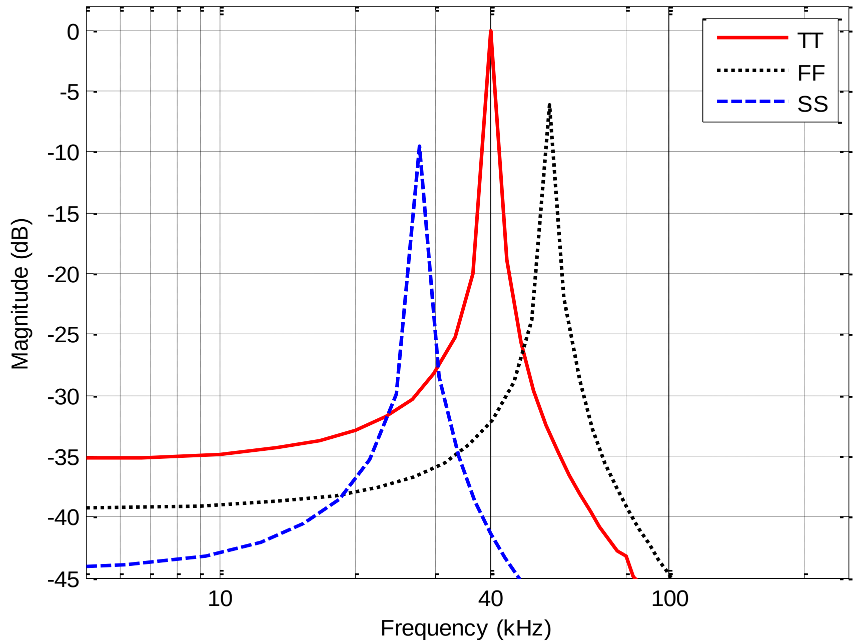

Figure 4.19 Frequency spectrum of 40-kHz oscillator at process corners

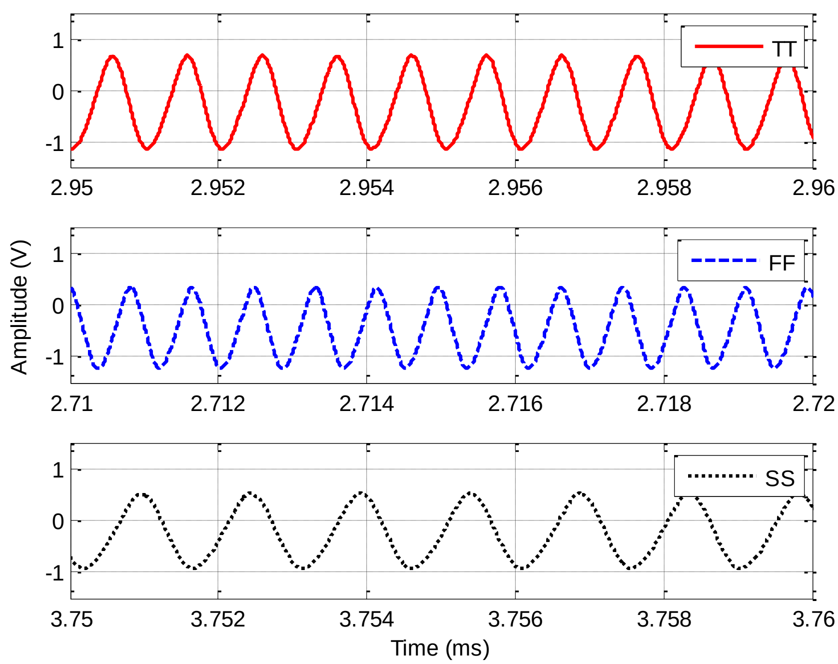

Figure 4.20 Time-domain output of 1-MHz sinusoidal oscillator at process corners

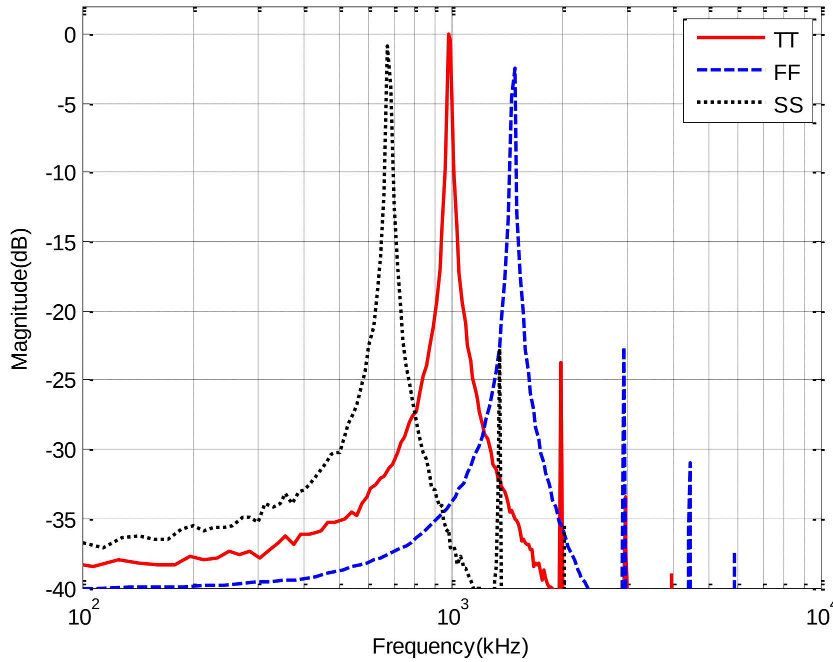

Figure 4.21 Frequency spectrum of 1-MHz sinusoidal oscillator at process corners

Table 4.9 Sinusoidal oscillators at different process corners

		TT	FF	SS
40-kHz Oscillator	Frequency (kHz)	40.0	53.0	27.4
1-MHz Oscillator	Frequency (MHz)	0.99	1.35	0.67
	THD (%)	7.78	10.03	7.40

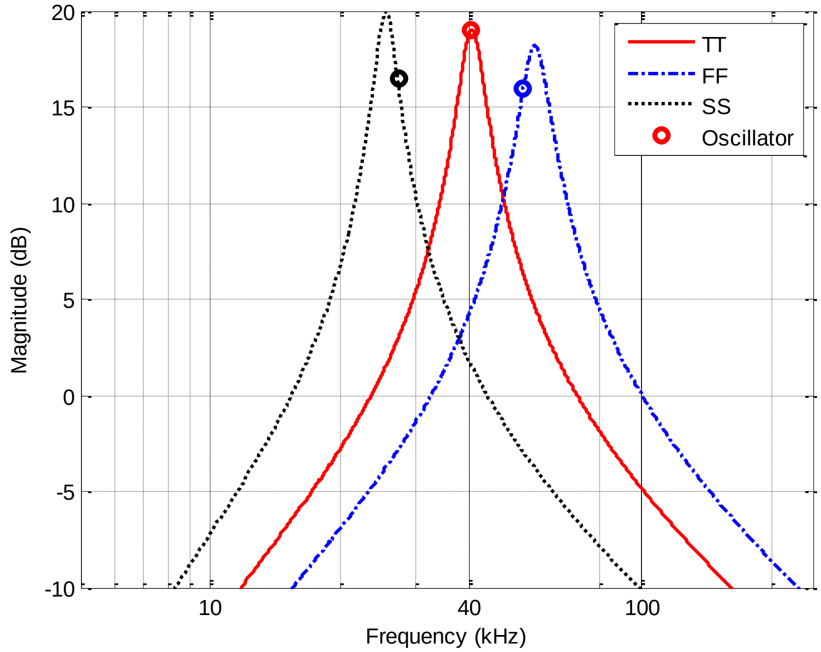

Figure 4.22 Frequency response of the 40-kHz pair at process corners

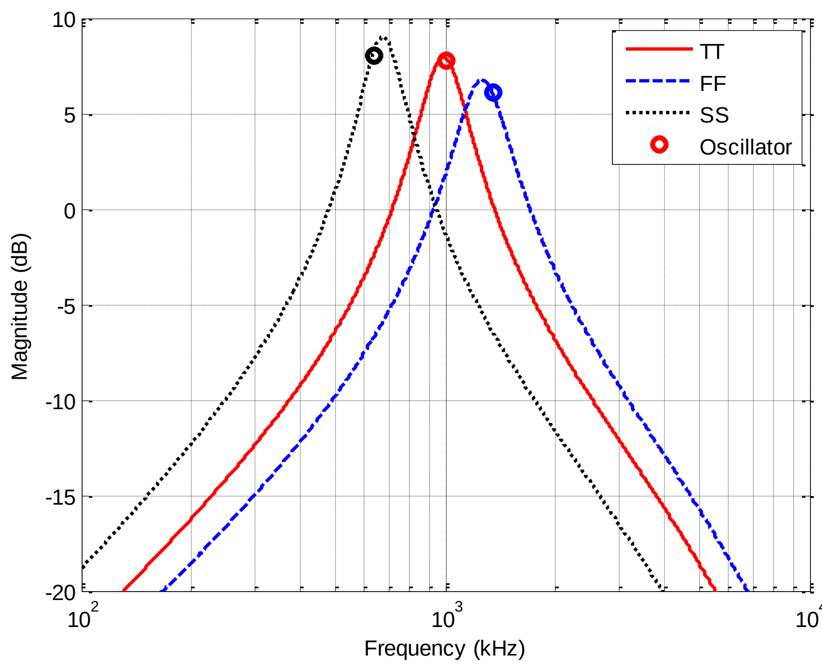

Figure 4.23 Frequency response of the 1-MHz pair at process corners

CHAPTER V

CONCLUSIONS

5.1 Summary

Two tuned bandpass filter and sinusoidal oscillator pairs are designed using the standard g_m-C architecture in a 0.5-μm technology. A design method for temperature compensation of an OTA using an all-CMOS temperature-dependent voltage source is introduced. The temperature compensation is accomplished by using a temperature-dependent circuit to bias the tail current source of the OTA. The temperature-compensated OTAs are used to construct a frequency-tuned bandpass filter and oscillator pair. The mismatch in the frequency characteristics of the pair are shown in simulation to remain lower than 6% over the temperature range from 25°C to 125°C. The all-CMOS architecture can be implemented inexpensively with no off-chip components.

5.2 Future work

The next steps in the design flow are the circuit layout and the fabrication of the proposed design. The performance of the tuned pairs of bandpass filters and sinusoidal oscillators at a particular process corner can be analyzed more accurately when the fabricated circuits are tested. The temperature-insensitive OTAs designed using the proposed method can be used to construct high-frequency bandpass filters and sinusoidal oscillators. The behavior of high-frequency bandpass filters and sinusoidal oscillators at higher temperatures can be studied using these bandpass filters and oscillators. Similarly, higher-order filters and oscillators may be constructed using the proposed OTAs and their performance at higher temperatures may be analyzed.

BIBLIOGRAPHY

1. M.E. Van Valkenburg and R. Schaumann, *Design of Analog Filters,* Oxford University Press, 2001.

2. A.S. Sedra and K.C. Smith, *Microelectronic Circuits,* Oxford University Press, 2004.

3. Y. Tsividis, “Integrated Continuous-Time Filter Design – An Overview,” *IEEE Journal of Solid-State Circuits,* vol. 29, no. 3, pp. 166–176, March 1994.

4. H.S. Malvar and M. Luettgen, “Temperature Compensation of OTA-Based Filters and Amplifiers,” *Electronic Letters,* vol. 23, no. 17, pp. 890-891, 1987.

5. S. Kumar, A. Govil, A. Bhattacharyya and D. Dutta, “Wide-Range Tunable Bandpass Filter cum Sinusoidal Oscillator Using a New Current-Controlled Resistor,” *IEEE Transactions on Circuits and Systems,* vol. 2, pp. 220-223, July 1999.

6. W. Surakampontorn, et al., “Temperature-Insensitive Voltage-to-Current Converter and Its Applications,” *IEEE Transactions on Instrumentation and Measurement,* vol. 48, no. 6, December 1999.

7. S. Solis-Bustos, J. Silva-Martinez, F. Maloberti and E. Sanchez-Sinencio, “A 60-DB Dynamic Range CMOS Sixth-Order 2.4-Hz Low-Pass Filter for Medical Applications,” *IEEE Transactions on Circuits and Syststems-II,* vol. 47, pp. 1391-1398, December 2000.

8. R. Schaumann, *Fundamental Concepts and Tools for the Design of Linear Analog Filters,* Prentice-Hall, 1990.

9. A. Zolfaghari, A. Chan and B. Razavi, “Stacked Inductors and Transformers in CMOS Technology,” *IEEE Journal of Solid-State Circuits,* vol. 36, no. 4, April 2001.

10. E. Sánchez-Sinencio and J. Silva-Martinez, “CMOS Transconductance Amplifiers, Architecture and Active Filters: a Tutorial,” *Proceedings of IEEE Circuits, Devices and Systems,* vol. 147, no. 1, pp. 3-12, February 2000.

11. B. Linares-Barranco, et al., “CMOS OTA-C High-Frequency Sinusoidal Oscillators,” *IEEE Journal of Solid-State Circuits,* vol. 26, no. 2, pp. 160-165, February 1991.

12. B. Razavi, *Design of Analog CMOS Integrated Circuits*, McGraw Hill, 2001.

13. A. Lewinski and J. Silva-Martinez, "OTA Linearity Enhancement Technique for High Frequency Applications with IM3 Below -65 dB, " *IEEE Transactions on Circuits and Systems—II: Express Briefs*, vol. 51, no. 10, October 2004

14. T. Lo and C. Hung, *1V CMOS Gm-C Filters: Design and Applications*, Springer, Analog Circuits and Signal Processing, 2009.

15. N. Talebbeydokhti, et al., "Constant Transconductance Bias Circuit with an On-Chip Resistor," *ISCAS Proceedings*, *IEEE International Symposium on Circuits and Systems*, pp. 2857–2860, May 2006

16. B.R. Gregoire and U. Moon, "A Sub 1-V Gm-C Switched–Capacitor Current Source," *IEEE Transactions on Circuits and Systems-II: Express Briefs*, vol. 54, no. 3, pp. 222–226, March 2007.

17. R. Dehghani and S. Atarodi, "A New Low Voltage Precision CMOS Current-Reference with No External Components," *IEEE Transactions on Circuits and Systems-II*, vol. 50, no. 12, pp. 938-942, December 2003.

18. W.M. Sansen, et al., "A CMOS Temperature-Compensated Current Reference," *IEEE Journal of Solid-State Circuit*s, vol. SC-23, pp. 821-824, June 1988.

19. I.M. Filanovsky and A. Allam, "Mutual Compensation of Mobility and Threshold Voltage Temperature Effects with Applications in CMOS Circuits," *IEEE Transactions on Circuits and Systems-I*, vol. 48, no. 7, pp. 876–883, July 2001.

20. Z. Prijic, et al., "Zero-temperature-coefficient (ZTC) Biasing of Power VDMOS Transistors," *Electronics Letters*, vol. 29, no. 5, pp. 435 – 437, March 1993.